Limit order trading with a mean reverting reference price

Saran Ahuja*, George Papanicolaou†, Weiluo Ren‡, and Tzu-Wei Yang§

Abstract. Optimal control models for limit order trading often assume that the underlying asset price is a Brownian motion since they deal with relatively short time scales. The resulting optimal bid and ask limit order prices tend to track the underlying price as one might expect. This is indeed the case with the model of Avellaneda and Stoikov (2008), which has been studied extensively. We consider here this model under the condition when the underlying price is mean reverting. Our main result is that when time is far from the terminal, the optimal price for bid and ask limit orders is constant, which means that it does not track the underlying price. Numerical simulations confirm this behavior. When the underlying price is mean reverting, then for times sufficiently far from terminal, it is more advantageous to focus on the mean price and ignore fluctuations around it. Mean reversion suggests that limit orders will be executed with some regularity, and this is why they are optimal. We also explore intermediate time regimes where limit order prices are influenced by the inventory of outstanding orders. The duration of this intermediate regime depends on the liquidity of the market as measured by specific parameters in the model.

Key words. limit order trading, optimal execution, stochastic optimal control, mean reverting prices

1. Introduction. Limit orders play an essential role in today's financial markets. How to optimally submit limit orders has therefore become an important research area. Limit order traders set the price of their orders, and the market determines how fast their orders are executed. Avellaneda and Stoikov proposed a stochastic control model [3] for a single limit order trader that optimizes an expected terminal utility of portfolio wealth. In this model, market orders are given by a Poisson flow with rate $A\exp(-\kappa\delta)$ where δ is the spread between the limit order price and the observed underlying reference price, while A and κ are two positive parameters that control the speed of execution, reflecting in this way the liquidity of the market. The assumption of a Poisson flow is based on two empirical facts presented and discussed in [25, 27, 40, 47, 51]. One is that in equity markets the distribution of the size of market orders is consistent with a power law, and the other is that the change in the depth of the limit order book caused by one market order is proportional to the logarithm of the size of that order. The Avellaneda-Stoikov model is formulated as a stochastic optimal control problem where the trader balances limit order prices and trading frequency to maximize the expected exponential terminal utility of wealth.

The approach of Avellaneda and Stoikov has been analyzed and extended in [15, 19, 29–31, 52]. In this paper, we use the same optimal control problem, but we are interested in longer time scales. On a short time scale, the reference price can be modeled by a Brownian motion as seems appropriate in high frequency trading. On a longer time scale corresponding to intermediate trading frequency, we may assume a mean reverting reference price modeled by an Ornstein-Uhlenbeck (OU) process. Reviews of mean reverting behavior in equity markets

*Department of Mathematics, Stanford University, Stanford, CA 94305 (ssunny@stanford.edu)
†Department of Mathematics, Stanford University, Stanford, CA 94305 (papanico@math.stanford.edu)
‡Department of Mathematics, Stanford University, Stanford, CA 94305 (weiluo@stanford.edu)
§School of Mathematics, University of Minnesota, Minneapolis, MN 55455 (yangx953@umn.edu)

and associated time scales are presented in [22, 34].

In this paper, we present a numerical study of the long-time limit of the optimal limit order prices in the Avellaneda and Stoikov model with an OU price process. In addition, we study analytically the equilibrium value function of the optimal control problem. Long time behavior of a limit order control problem is studied by Gueant, Lehalle, and Fernandez-Tapia [30]. They use the Avellaneda and Stoikov model but with a Brownian motion price process instead of a mean reverting one. They impose inventory limits which, after some transformations, reduce the problem to a finite-dimensional system of ordinary differential equations. They show that the optimal spreads converge to inventory-dependent limits when time is far away from terminal. Zhang [52] and Fodra and Labadie [19, 20] also study the Avellaneda and Stoikov model with an OU price process, although they do not consider the long time limit of the trader's optimal strategy. Fodra and Labadie analyze the case where the reference price is away from its long term mean. The trader then anticipates and takes advantage of the tendency of the price to go back to the long term mean. In this paper we are interested in how the trader would behave if he/she expects that the reference price is likely to oscillate around its long term mean for a relatively long time. We are interested in the case in which the trading period consists of multiple mean reversion cycles of the reference price, while Fodra and Labadie [19] consider one or just a half of such a cycle.

Our main result is that the optimal limit order prices, instead of the optimal spreads, converge to limits that are independent of all the state variables in the model. This is shown numerically by two different computational methods. The limit value function is also studied analytically. In addition, we observe numerically that the speed at which the optimal limit order prices become insensitive to the reference price is different from that of the inventory levels: the former converges much faster. When the trading period is sufficiently long, we observe roughly three stages in the optimal trading strategy:

1. Far from the terminal time, the trader uses constant limit order prices to generate profit with little concern for risk aversion or leftover inventory.
2. At intermediate times, the trader maintains inventory levels by posting limit orders that depend on inventory levels.
3. Near the terminal time, the trading behavior is mostly determined by the exponential utility function.

We observe that in certain parameter regimes when time is away from terminal by several mean reversion cycles of the reference price, the trader updates limit order prices only according to the change of inventory levels. These changes become smaller as time moves backwards and are effectively zero when time is far away from the terminal time, in which case the trader posts constant limit order prices. Near the terminal time, the optimal limit order prices are affected by the long-term variance of the reference price and the exponential terminal utility function. We also observe that, with other parameters fixed, the optimal limit order prices converge to their long-term limits faster when the market has more liquidity, which in this model is controlled by parameters in the Poisson flow of orders.

We note that when the trader posts constant limit order prices, then wealth accumulates from the difference between the buy-sell limit order prices instead of from the difference between these prices and the reference price. This strategy is somewhat analogous to a pairs trading strategy, and when the trading period is long enough, it appears to beat the strategy of

tracking the reference price. However, by posting constant limit order prices, the trader gives up the ability to control the trading rate, which is determined entirely by the fluctuations of the reference price. As a result, the variance of the inventory is large, and this is not desirable near the end of the trading period due to the terminal exponential utility. Therefore, before getting close to the end of the trading period, the trader needs to keep track of the reference price so as to control the trading flow and avoid a large leftover inventory.

By linearizing the exponential trading intensity, the Avellaneda and Stoikov model with an OU reference price is reduced to a model that can be solved analytically. This is done in Zhang [52] and also in Fodra and Labadie [19]. We compare our numerical solutions with the approximation in Zhang [52] and find good agreement when time is not too far away from terminal.

The structure of this paper is as follows: We first present the model in Section 2, then introduce the numerical methods used in Section 3. The numerical methods are discussed in detail in the appendix. In Section 4 and 5, we discuss our results for the long-time behavior of the optimal limit order prices and compare them with what is expected analytically. We do not have a full analytical treatment of the long-time behavior of the HJB equation at present. However, in Section 6, we carry out an equilibrium analysis on the (time-independent) HJB equation and compare the analytical results obtained with those of our long-time numerical simulations. The result confirms the accuracy of our numerical methods.

2. Trading model.

2.1. Settings. We assume that the reference price S_t of the risky asset follows an Ornstein-Uhlenbeck (OU) process

$$dS_t = \alpha\left(\mu - S_t\right)dt + \sigma dB_t \tag{1}$$

where α is the mean-reverting rate, μ is the long-term mean, and σ is the volatility. Note that we are not considering any feedback effect of traders' behavior on the reference price here.

The portfolio of the limit trader consists of two parts: cash and the risky asset. We denote the cash process by X_t and the inventory process of the risky asset by Q_t. The process Q_t can be expressed as the difference of ask and bid limit orders fulfilled up to time t, denoted by Q_t^a and Q_t^b:

$$Q_t = Q_t^b - Q_t^a + q_0, \tag{2}$$

assuming that the trader only post limit orders and q_0 is the initial inventory. The portfolio is self-financing, so

$$dX_t = p_t^a dQ_t^a - p_t^b dQ_t^b, \tag{3}$$

where p_t^a and p_t^b are the ask and bid limit prices respectively. Gathering (1), (2) and (3), the dynamics of variables in our model are

$$\begin{cases} dQ_t = dQ_t^b - dQ_t^a \\ dX_t = p_t^a dQ_t^a - p_t^b dQ_t^b \\ dS_t = \alpha\left(\mu - S_t\right)dt + \sigma dB_t \end{cases} \tag{4}$$

Note that p_t^a and p_t^b are the controls of the limit order trader, while the processes of the fulfilled limit orders Q_t^a and Q_t^b may be affected by those limit order prices as well as the reference price S_t.

Combining empirical results from econophysics in [25,27,40,47,51], Avellaneda and Stoikov proposed that the process of the fulfilled limit orders follows a doubly stochastic Poisson process with intensity $Ae^{-\kappa\delta_t}$, where δ_t is the spread of the limit order at time t, and A and κ are positive constants characterizing statistically the liquidity of the asset. Namely

$$\begin{cases} Q_t^b \sim \text{Poi}\left(Ae^{-\kappa\delta_t^b}\right) \\ Q_t^a \sim \text{Poi}\left(Ae^{-\kappa\delta_t^a}\right) \end{cases} \tag{5}$$

where $\delta_t^b = S_t - p_t^b$ and $\delta_t^a = p_t^a - S_t$ are the spread of ask and bid limit orders posted at time t.

The trader aims to solve the optimal control problem

$$\sup_{\delta^a,\delta^b} E\left[-e^{-\gamma W_T}\right]. \tag{6}$$

where $W_t = X_t + Q_t S_t$ is the process of total wealth.

The parameters in our model are

$$\begin{cases} A\text{: the magnitude of market order flow;} \\ \kappa\text{: dictating the shape of order book;} \\ \gamma\text{: risk-aversion factor;} \\ \alpha\text{: the mean reverting rate of the reference price;} \\ \sigma\text{: the volatility of the reference price;} \\ T\text{: the length of the trading period.} \end{cases} \tag{7}$$

2.2. Dynamic programming. Consider the value function

$$u(t,q,x,s) = \sup_{\delta^a,\delta^b} E\left(-e^{-\gamma W_T} | Q_t = q, X_t = x, S_t = s\right). \tag{8}$$

The HJB equation for the optimal control problem specified in (4) (5) and (6) is

$$\begin{aligned} 0 = u_t + \frac{\sigma^2}{2} u_{ss} + \alpha(\mu - s) u_s + \sup_{\delta^a,\delta^b} \Big\{ & \\ & \left[u(t,q-1,x+s+\delta^a,s) - u(t,q,x,s)\right] Ae^{-\kappa\delta^a} + \\ & \left[u\left(t,q+1,x-s+\delta^b,s\right) - u(t,q,x,s)\right] Ae^{-\kappa\delta^b} \Big\} \end{aligned} \tag{9}$$

with the terminal condition

$$u(T,q,x,s) = -e^{-\gamma(x+qs)}. \tag{10}$$

Because of the special form of the terminal utility, namely the CARA[1] utility, it is known from the studies in Zhang [52] and Gueant, Lehalle, and Fernandez-Tapia [30] that the ansatz $u(t,q,x,s) = -e^{-\gamma(x+v(t,q,s))}$ can reduce (9) to

$$\begin{aligned} 0 =& v_t - \frac{\sigma^2}{2}\left(\gamma v_s^2 - v_{ss}\right) + \alpha(\mu - s) v_s \\ &+ \frac{1}{\gamma}\sup_{\delta^a,\delta^b}\Big[\left(1 - e^{-\gamma(s+\delta^a+v(t,s,q-1)-v(t,s,q))}\right) Ae^{-\kappa\delta^a} \\ &+ \left(1 - e^{-\gamma\left(-s+\delta^b+v(t,s,q+1)-v(t,s,q)\right)}\right) Ae^{-\kappa\delta^b}\Big] \end{aligned} \tag{11}$$

with terminal condition

$$v(T,q,s) = qs. \tag{12}$$

To find the optimal feedback control, we only need to maximize

$$\begin{aligned} F^a(\delta^a) &= \left(1 - e^{-\gamma(s+\delta^a+v(t,s,q-1)-v(t,s,q))}\right) Ae^{-\kappa\delta^a} \\ F^b\left(\delta^b\right) &= \left(1 - e^{-\gamma\left(-s+\delta^b+v(t,s,q+1)-v(t,s,q)\right)}\right) Ae^{-\kappa\delta^b} \end{aligned} \tag{13}$$

separately. Both F^a and F^b have a unique global maximum which yields the optimal feedback spreads

$$\begin{aligned} \delta^{a*}(t,q,s) &= \frac{1}{\gamma}\log\left(1+\frac{\gamma}{\kappa}\right) - s - v(t,q-1,s) + v(t,q,s), \\ \delta^{b*}(t,q,s) &= \frac{1}{\gamma}\log\left(1+\frac{\gamma}{\kappa}\right) + s - v(t,q+1,s) + v(t,q,s). \end{aligned} \tag{14}$$

Therefore the problem is reduced to solving the HJB equation

$$\begin{aligned} 0 =& v_t - \frac{\sigma^2}{2}\left(\gamma v_s^2 - v_{ss}\right) + \alpha(\mu - s) v_s \\ &+ \frac{1}{\gamma}\Big[\left(1 - e^{-\gamma(s+\delta^{a*}+v(t,s,q-1)-v(t,s,q))}\right) Ae^{-\kappa\delta^{a*}} \\ &+ \left(1 - e^{-\gamma\left(-s+\delta^{b*}+v(t,s,q+1)-v(t,s,q)\right)}\right) Ae^{-\kappa\delta^{b*}}\Big] \end{aligned} \tag{15}$$

with the terminal condition in (12) and the optimal controls in (14).

We make a change of time $\tau := T - t$ in (15), and define $\tilde{v}(\tau,q,s) = v(T-t,q,s)$. We abuse the notation by still using v instead of $\tilde{v}$. Plugging the optimal controls to (14), we have

$$\begin{aligned} v_\tau =& \frac{\sigma^2}{2}\left(v_{ss} - \gamma v_s^2\right) + \alpha(\mu - s) v_s + \\ & \frac{A}{\kappa+\gamma}\left(1+\frac{\gamma}{\kappa}\right)^{-\frac{\kappa}{\gamma}}\left(e^{-\kappa(-s-v(\tau,q-1,s)+v(\tau,q,s))} + e^{-\kappa(s-v(\tau,q+1,s)+v(\tau,q,s))}\right) \end{aligned} \tag{16}$$

[1] constant absolute risk aversion

with the initial condition

$$v(0,q,s) = qs. \tag{17}$$

Note that (16) is highly nonlinear because of the appearance of value function v in the exponent. Moreover, this equation involves both continuous variables, t and s, and a discrete variable q. There is no available theory on its well-posedness. On the other hand, for the case $\alpha = 0$, this equation can be transformed to an ODE system, which, under the assumption of finite inventory limits, is finite-dimensional and can be solved explicitly. See Zhang [52] or Gueant, Lehalle and Fernandez-Tapia [30] for detail.

2.3. Scaling. We will consider two scalings for our model: one on time and another one on price.

2.3.1. Time scaling. Consider a scaled time

$$\tilde{t} = \frac{t}{K} \tag{18}$$

which would be dimensionless if the dimension of K is the one of time. In particular, we choose $K = \frac{1}{\alpha}$, in which case the dimensionless $\tilde{t}$ represents the number of mean reversion cycles of the reference price. That is, we set

$$\tilde{t} = \alpha t \Longleftrightarrow t = \frac{\tilde{t}}{\alpha} \tag{19}$$

Let $\left(Q_t, X_t, S_t, \delta_t^a, \delta_t^b\right)$ denote a solution of the stochastic control problem (4) and (6). Define

$$\begin{cases} \tilde{Q}_{\tilde{t}} = Q_t = Q_{\frac{\tilde{t}}{\alpha}} \\ \tilde{X}_{\tilde{t}} = X_t = X_{\frac{\tilde{t}}{\alpha}} \\ \tilde{S}_{\tilde{t}} = S_t = S_{\frac{\tilde{t}}{\alpha}} \\ \tilde{\delta}_{\tilde{t}}^a = \delta_t^a = \delta_{\frac{\tilde{t}}{\alpha}}^a \\ \tilde{\delta}_{\tilde{t}}^b = \delta_t^b = \delta_{\frac{\tilde{t}}{\alpha}}^b \end{cases} \tag{20}$$

which satisfy

$$\begin{cases} \tilde{Q}_{\tilde{t}}^b \sim \text{Poi}\left(\frac{A}{\alpha} e^{-\kappa \tilde{\delta}_{\tilde{t}}^b}\right) \\ \tilde{Q}_{\tilde{t}}^a \sim \text{Poi}\left(\frac{A}{\alpha} e^{-\kappa \tilde{\delta}_{\tilde{t}}^a}\right) \\ d\tilde{Q}_{\tilde{t}} = d\tilde{Q}_{\tilde{t}}^b - d\tilde{Q}_{\tilde{t}}^a \\ d\tilde{X}_{\tilde{t}} = \left(\tilde{\delta}_{\tilde{t}}^a + \tilde{S}_{\tilde{t}}\right) \tilde{Q}_{\tilde{t}}^a - \left(\tilde{S}_{\tilde{t}} - \tilde{\delta}_{\tilde{t}}^b\right) \tilde{Q}_{\tilde{t}}^b \\ d\tilde{S}_{\tilde{t}} = \left(\mu - \tilde{S}_{\tilde{t}}\right) d\tilde{t} + \frac{\sigma}{\sqrt{\alpha}} d\tilde{B}_{\tilde{t}} \\ \sup\limits_{\tilde{\delta}^a, \tilde{\delta}^b} E\left[-e^{-\gamma\left(\tilde{X}_{\alpha T} + \tilde{Q}_{\alpha T} \tilde{S}_{\alpha T}\right)}\right] \end{cases} \tag{21}$$

We will use the new variables in (20) and the following new parameters

$$\begin{cases} \tilde{A} = \frac{A}{\alpha} \\ \tilde{\alpha} = 1 \\ \tilde{\sigma} = \frac{\sigma}{\sqrt{\alpha}} \\ \tilde{T} = \alpha T \end{cases} \tag{22}$$

while abusing the notation by dropping all the tildes. The resulting system is almost identical to the one in (4), (5), and (6) except that we drop the parameter α since it is always equal to one after time-scaling.

With the new set of parameters after scaling, equation (16) together with the initial condition becomes

$$\begin{cases} 0 = v_\tau + \frac{\sigma^2}{2}\left(\gamma v_s^2 - v_{ss}\right) - (\mu - s)\, v_s \\ \qquad - \frac{A}{\kappa+\gamma}\left(1 + \frac{\gamma}{\kappa}\right)^{-\frac{\kappa}{\gamma}} \left(e^{-\kappa(-s-v(\tau,q-1,s)+v(\tau,q,s))} + e^{-\kappa(s-v(\tau,q+1,s)+v(\tau,q,s))}\right) \\ v\,(0,q,s) = qs \end{cases} \tag{23}$$

Note that, in general a time-scaling with scaling factor K would transform the control problem with parameter A, α, σ and T to the one with parameters KA, $K\alpha$, $\sqrt{K}\sigma$, and T/K.

2.3.2. Price scaling. Now we consider a scaling on all the price-related quantities to make them dimensionless. Note that the dimension of parameter γ is the reciprocal of that of price, so γS_t is dimensionless, and so are γX_t, $\gamma \delta_t^a$ and $\gamma \delta_t^b$. Define

$$\begin{cases} \tilde{X}_t = \gamma X_t \\ \tilde{S}_t = \gamma S_t \\ \tilde{\delta_t^a} = \gamma \delta_t^a \\ \tilde{\delta_t^b} = \gamma \delta_t^b \end{cases} \tag{24}$$

which satisfy

$$\begin{cases} dQ_t = dQ_t^b - dQ_t^a \\ d\tilde{X}_t = \left(\tilde{S}_t + \tilde{\delta}_t^a\right) dQ_t^a - \left(\tilde{S}_t - \tilde{\delta}_t^b\right) dQ_t^b \\ d\tilde{S}_t = \left(\gamma\mu - \tilde{S}_t\right) dt + \gamma\sigma dB_t \\ Q_t^b \sim \text{Poi}\left(Ae^{-\frac{\kappa}{\gamma}\tilde{\delta}_t^b}\right) \\ Q_t^a \sim \text{Poi}\left(Ae^{-\frac{\kappa}{\gamma}\tilde{\delta}_t^a}\right) \\ \sup\limits_{\tilde{\delta}^a, \tilde{\delta}^b} E\left[-e^{-\left(\tilde{X}_T + \tilde{S}_T Q_T\right)}\right]. \end{cases} \tag{25}$$

Now we define a new set of parameters

$$\begin{cases} \tilde{\mu} = \gamma\mu, \\ \tilde{\sigma} = \gamma\sigma, \\ \tilde{\kappa} = \frac{\kappa}{\gamma}. \end{cases} \tag{26}$$

Once again, we use the new variables and parameters but drop all the tildes. This leads to the following system:

$$
\begin{cases}
dQ_t = dQ_t^b - dQ_t^a \\
dX_t = \left(S_t + \delta_t^a\right) dQ_t^a - \left(S_t - \delta_t^b\right) dQ_t^b \\
dS_t = \left(\mu - S_t\right) dt + \sigma dB_t \\
Q_t^b \sim \text{Poi}\left(Ae^{-\kappa\delta_t^b}\right) \\
Q_t^a \sim \text{Poi}\left(Ae^{-\kappa\delta_t^a}\right) \\
\sup\limits_{\delta^a,\delta^b} E\left[-e^{-(X_T+S_TQ_T)}\right].
\end{cases}
\tag{27}
$$

In the new system, all the price-related quantities are dimensionless as they are measured relative to the magnitude of trader's risk aversion. Here we drop another variable γ, for the fact that it is always equal to one after price-scaling. Repeating all the steps in section 2.2, we have the HJB equation

$$
\begin{cases}
0 = v_\tau + \frac{\sigma^2}{2}\left(v_s^2 - v_{ss}\right) - \left(\mu - s\right) v_s \\
\qquad -\frac{A}{\kappa+1}\left(1+\frac{1}{\kappa}\right)^{-\kappa}\left(e^{-\kappa(-s-v(\tau,q-1,s)+v(\tau,q,s))} + e^{-\kappa(s-v(\tau,q+1,s)+v(\tau,q,s))}\right) \\
v\left(0,q,s\right) = qs
\end{cases}
\tag{28}
$$

for $v(t,q,s)$ satisfying $e^{-(x+v)} = \sup\limits_{\delta^a,\delta^b} E\left(e^{-(X_T+S_TQ_T)}|X_t = x, S_t = s, Q_t = q\right)$. The optimal feedback controls are given by

$$
\begin{aligned}
\delta^{a*}\left(t,q,s\right) &= \log\left(1+\frac{1}{\kappa}\right) - s - v\left(t,q-1,s\right) + v\left(t,q,s\right) \\
\delta^{b*}\left(t,q,s\right) &= \log\left(1+\frac{1}{\kappa}\right) + s - v\left(t,q+1,s\right) + v\left(t,q,s\right)
\end{aligned}
\tag{29}
$$

From now on, we will only consider the model in (27), the HJB equation in (28), and optimal feedback controls in (29). However, when showing our numerical simulation results, we would use the prices before the price-scaling, which are directly observable from the market, instead of the dimensionless ones after the scaling. For the parameters used in the numerical simulations, we may also choose the ones before the price-scaling, since they are easier to reason and are practically easier to calibrate to market data.

We point out that

1. After the price-scaling, the price-related quantities S_t, X_t, δ_t^a, δ_t^b, μ and σ in (27) are not observable as in (4) and (5). Instead, they are dimensionless and measured in the scale of the trader's risk aversion level.
2. The function v and variable s in (28) and (29) are actually γv and γs in terms of γ, v, and s before the price-scaling.
3. The optimal controls in (29) are the ones in (14) scaled by γ.

4. After both time and price scaling, we are using the following new set of parameters but abusing the notation by dropping all the tildes.

$$\begin{cases} \tilde{A} = \frac{A}{\alpha} \\ \tilde{\alpha} = 1 \quad \text{(It would be omitted in the new system.)} \\ \tilde{\sigma} = \gamma \frac{\sigma}{\sqrt{\alpha}} \\ \tilde{\mu} = \gamma \mu, \\ \tilde{\kappa} = \frac{\kappa}{\gamma} \\ \tilde{\gamma} = 1 \quad \text{(It would also be omitted in the new system.)} \\ \tilde{T} = \alpha T \end{cases} \tag{30}$$

where the parameters on the right hand side of equations are from (7), namely the ones in the original setting without any scaling.

In the subsequent sections, when discussing how the parameters would affect the model, we will be referring to the new parameters after the scaling instead of those in (7). Note that even though we dropped two parameters, namely α and γ, we have not lost any generality after those two scalings. For a model in (4), (5), and (6) with an arbitrary group of parameters, we can solve a model in (27) with scaled parameters constructed in (30), then convert it to a solution of the original model before scalings.

3. Numerical methods.

We briefly discuss two numerical methods that we will use to solve the optimal stochastic control problem described in section 2, particularly equation (28), and produce all the results discussed in the subsequent sections.

The first method is a fully-implicit finite difference scheme. This method has advantages of being relatively simple to implement and numerically stable. However, it can be slow due to the iteration required at each time steps. See Appendix A for the detail on the discretization and iteration step.

Secondly, we implement what is called a split-step scheme which performs the numerics separately between the linear and nonlinear part of the equation. We briefly describe the method here and provide more detail in Appendix A.

We consider the following transformation of the value function v in (28)

$$\tilde{v} = e^{-v} \tag{31}$$

which satisfies

$$\begin{cases} \tilde{v}_\tau = (\mu - s)\, \tilde{v}_s + \frac{\sigma^2}{2} \tilde{v}_{ss} - \frac{A}{\kappa+1} \left(A e^{-\kappa \delta^{a*}} + A e^{-\kappa \delta^{b*}} \right) \tilde{v} \\ \tilde{v}(0, q, s) = e^{-qs} \end{cases} \tag{32}$$

where

$$\begin{aligned} \delta^{a*}(\tau, q, s) &= -s + \left[\log\left(1 + \frac{1}{\kappa}\right) + \log \tilde{v}(\tau, q-1, s) - \log \tilde{v}(\tau, q, s) \right] \\ \delta^{b*}(\tau, q, s) &= s + \left[\log\left(1 + \frac{1}{\kappa}\right) + \log \tilde{v}(\tau, q+1, s) - \log \tilde{v}(\tau, q, s) \right] \end{aligned} \tag{33}$$

We split the PDE in (32) to two PDEs:

$$\tilde{v}_\tau = (\mu - s)\,\tilde{v}_s + \frac{\sigma^2}{2}\tilde{v}_{ss} \tag{34}$$

and

$$\tilde{v}_\tau = -\frac{A}{\kappa+1}\left(Ae^{-\kappa\delta^{a*}} + Ae^{-\kappa\delta^{b*}}\right)\tilde{v} \tag{35}$$

Here equation (34) can be solved via the Feymann-Kac formula, and equation (35) can be solved exactly using the method in Zhang [52] if we impose finite inventory limits for our problem, in which case the transformation

$$w(t,s,q) = e^{-\kappa s q}\tilde{v}^{-\kappa} \tag{36}$$

reduces (35) to a finite-dimensional ODE system that can be solved using a matrix exponential of a tri-diagnoal matrix. Combining those two steps, we have devised a split-step scheme to solve (32). Again, see Appendix A for detail.

The feedback optimal limit prices produced by these two methods match very well if we discretize the time space and reference-price space properly. Compared to the finite difference method, the split-step method is much faster since there is no iteration involved. Moreover, the split-step used the Feymann-Kac formula dealing with the mean reversion feature in the model, which is fully implicit, stable and suitable for observing the long time behavior. However, because of (31), the function $\tilde{v}$ may face an underflow/overflow issue when the absolute value of function v is large, which would be the case if we allow large s or q in our computation or use fairly large parameters. Therefore, compared to the split-step method, the finite difference method can be applied to a wider range of parameters.

4. Long time behavior. Studying standard Avellaneda-Stoikov model, Gueant, Lehalle, and Fernandez-Tapia [30] observed a long-term stationary behavior of the optimal spreads δ_t^{a*} and δ_t^{b*}:

$$\begin{aligned} \lim_{T-t\to\infty} \delta^{a*}(t,q) &= \delta_\infty^{a*}(q) \\ \lim_{T-t\to\infty} \delta^{b*}(t,q) &= \delta_\infty^{b*}(q) \end{aligned} \tag{37}$$

See the appendix for a brief summary.

In our model, we observe a long-time behavior of the optimal limit order prices $p_t^{a*} = S_t + \delta_t^{a*}$ and $p_t^{b*} = S_t - \delta_t^{b*}$ instead of that of the optimal spreads δ_t^{a*} and δ_t^{b*}.

Our numerical simulations presented in section 5 indicate that the optimal feedback limit order prices given by

$$\begin{aligned} p^{a*}(\tau,q,s) &= \log\left(1+\frac{1}{\kappa}\right) - v(\tau,q-1,s) + v(\tau,q,s) \\ p^{b*}(\tau,q,s) &= -\log\left(1+\frac{1}{\kappa}\right) + v(\tau,q+1,s) - v(\tau,q,s) \end{aligned} \tag{38}$$

converge to constants

$$
\begin{aligned}
p_{\infty}^{a*} &= \mu + \log\left(1 + \frac{1}{\kappa}\right) \\
p_{\infty}^{b*} &= \mu - \log\left(1 + \frac{1}{\kappa}\right)
\end{aligned}
\tag{39}
$$

when $\tau \to \infty$. Equivalently,

$$
\lim_{\tau \to \infty} v\left(\tau, q, s\right) - v\left(\tau, q-1, s\right) = \mu. \tag{40}
$$

Note that the limits in (39) do not depend on either q or s, while those in (37) do depend on q. Moreover, Equation (37) considers limits of optimal spreads instead of those of optimal limit order prices. If we consider the limit of optimal limit prices in the standard Avellaneda-Stoikov model with finite inventory constraint, then it would be

$$
\begin{aligned}
p_{\infty}^{a*}(s, q) &= s + \delta_{\infty}^{a*}(q) \\
p_{\infty}^{b*}(s, q) &= s - \delta_{\infty}^{b*}(q)
\end{aligned}
\tag{41}
$$

using notations in (37). Comparing (39) and (41), we see that, for our model with a mean-reverting reference price, the asymptotic optimal strategy is to use constant limit order prices ignoring both the inventory and the reference price, while in a model with a Brownian motion, the optimal strategy is to track the reference price with spreads depending only on the inventory.

We have not yet developed an analytical proof of the convergence in (40) as this is work in progress. Note that $v\left(0, q, s\right) = qs$, so v can be intuitively viewed as the value of the asset held by the trader at time $T - \tau$. The limiting property in (40) suggests that, in the long run, the value of each share of asset is just μ, the long term mean of the reference price. Moreover, the convergence suggests that when we are sufficiently far away from the terminal time, it is better to post constant limit prices than to track the reference price closely. One heuristic explanation is that the trading period is so long compared to the mean reversion time that plenty of rebalancing is guaranteed. Therefore, as long as the trader can gain the premium from rebalancing by using the constant limit ask and bid prices, he/she does not need to track the reference price.

In the rest of this section, we discuss three closely related models that can be solved analytically and compare the limit of the optimal limit prices in those models with the ones in (39). We also show, in the last subsection, that the strategy of posting constant prices in our model is loosely analogous to the pairs trading strategy.

4.1. Model with constant reference price. In our case, the final limit of the optimal prices does not depend on the long-term standard deviation of the reference price. Instead, it uses the spread $\log\left(1 + \frac{1}{\kappa}\right)$ relative to the long-term mean of the reference price. It turns out

that this spread is closely related to the following model with a constant reference price:

$$
\begin{cases}
Q_t^b \sim \text{Poi}\left(Ae^{-\kappa\delta_t^b}\right) \\
Q_t^a \sim \text{Poi}\left(Ae^{-\kappa\delta_t^a}\right) \\
dQ_t = dQ_t^b - dQ_t^a \\
dX_t = \left(\delta_t^a + S_t\right) dQ_t^a - \left(S_t - \delta_t^b\right) dQ_t^b \\
S_t \equiv \mu \\
Q_0 = q_0, \quad X_0 = x_0 \\
\sup\limits_{\delta^a,\delta^b} E\left[-e^{-(X_T+Q_T\mu)}\right].
\end{cases}
\tag{42}
$$

The HJB equation for this optimal control problem is

$$
\begin{aligned}
0 = u_t\left(t,x,q\right) &+ \sup_{\delta^b} Ae^{-\kappa\delta^b}\left[u\left(t, x - \left(\mu - \delta^b\right), q+1\right) - u\left(t,x,q\right)\right] \\
&+ \sup_{\delta^a} Ae^{-\kappa\delta^a}\left[u\left(t, x + \left(\mu + \delta^a\right), q-1\right) - u\left(t,x,q\right)\right]
\end{aligned}
\tag{43}
$$

with the terminal condition $u(T,x,q) = -e^{-(x+q\mu)}$. Considering the ansatz $u\left(t,x,q\right) = -e^{-x}v\left(t,q\right)$, then v satisfies

$$
v_t - \frac{A}{\kappa+1}\left(e^{-\kappa\delta^{b*}} + e^{-\kappa\delta^{a*}}\right)v = 0, \quad v\left(T,q\right) = e^{-\mu q}
\tag{44}
$$

with the optimal controls given by

$$
\begin{aligned}
\delta^{b*}\left(t,q\right) &= \mu + \left[\log\left(1+\frac{1}{\kappa}\right) + \log v\left(t,q+1\right) - \log v\left(t,q\right)\right] \\
\delta^{a*}\left(t,q\right) &= -\mu + \left[\log\left(1+\frac{1}{\kappa}\right) + \log v\left(t,q-1\right) - \log v\left(t,q\right)\right],
\end{aligned}
\tag{45}
$$

It is easy to check that

$$
v\left(t,q\right) = e^{-\mu q}e^{-M(T-t)}
\tag{46}
$$

where

$$
M = \frac{2A}{\kappa+1}\left(1+\frac{1}{\kappa}\right)^{-\kappa}.
\tag{47}
$$

gives a solution to (44). Plugging (46) into (45), we can see that the constants in (39) are the exact optimal limit prices, and that $\log\left(1+\frac{1}{\kappa}\right)$ is the exact optimal spread in this degenerate case.

4.2. Analysis of small κ. Both Fodra and Labadie [19] and Zhang [52] considered approximations of (28) with linearization. We briefly state Zhang's results here.

After a linearization of the exponential terms,

$$e^{-\kappa\delta^{a*}} \longrightarrow 1-\kappa\delta^{a*}, \quad e^{-\kappa\delta^{b*}} \longrightarrow 1-\kappa\delta^{b*}, \tag{48}$$

Zhang derived the following equation from (28).

$$\begin{cases} 0 = v_\tau + \frac{\sigma^2}{2}\left(v_s^2 - v_{ss}\right) - (\mu - s)\, v_s - \frac{A}{\kappa+1}\left[\left(1-\kappa\delta^{a*}\right) + \left(1-\kappa\delta^{b*}\right)\right] \\ v\left(0,s,q\right) = sq, \end{cases} \tag{49}$$

where δ^{a*} and δ^{b*} are given in (29), which we repeat here for reference.

$$\begin{aligned} \delta^{a*}\left(t,q,s\right) &= \log\left(1+\frac{1}{\kappa}\right) - s - v\left(t,q-1,s\right) + v\left(t,q,s\right) \\ \delta^{b*}\left(t,q,s\right) &= \log\left(1+\frac{1}{\kappa}\right) + s - v\left(t,q+1,s\right) + v\left(t,q,s\right). \end{aligned}$$

The solution of the linearized PDE can be decomposed as

$$v\left(\tau,s,q\right) = \zeta\left(\tau,q\right) + s\phi\left(\tau,q\right), \tag{50}$$

where

$$\begin{cases} \zeta\left(\tau,q\right) = \zeta_0\left(\tau\right) + \zeta_1\left(\tau\right)\cdot q - \frac{1}{2}\zeta_2\left(\tau\right)\cdot q^2 \\ \phi\left(\tau,q\right) = e^{-\tau}\cdot q \end{cases} \tag{51}$$

with

$$\begin{cases} \zeta_0\left(\tau\right) = \frac{2\kappa A}{(\kappa+1)}\left(\frac{1}{\kappa} - \log\left(1+\frac{1}{\kappa}\right)\right)\tau - \frac{\sigma^2\kappa A}{2(\kappa+1)}\cdot\left(e^{-2\tau} - 1 + 2\tau\right) \\ \zeta_1\left(\tau\right) = \mu\left(1-e^{-\tau}\right) \\ \zeta_2\left(\tau\right) = \sigma^2\cdot\frac{1-e^{-2\tau}}{2}. \end{cases} \tag{52}$$

So the optimal feedback spreads are given by

$$\begin{aligned} \delta^{a*}\left(\tau,q,s\right) &= \log\left(1+\frac{1}{\kappa}\right) - s + \zeta_1\left(\tau\right) - \frac{1}{2}\zeta_2\left(\tau\right)\left(2q-1\right) + se^{-\tau} \\ \delta^{b*}\left(\tau,q,s\right) &= \log\left(1+\frac{1}{\kappa}\right) + s - \zeta_1\left(\tau\right) + \frac{1}{2}\zeta_2\left(\tau\right)\left(2q+1\right) - se^{-\tau} \end{aligned} \tag{53}$$

and, in turn, the optimal feedback prices are given by

$$\begin{aligned} p^{a*}\left(\tau,q,s\right) &= \log\left(1+\frac{1}{\kappa}\right) + \zeta_1\left(\tau\right) - \frac{1}{2}\zeta_2\left(\tau\right)\left(2q-1\right) + se^{-\tau} \\ p^{b*}\left(\tau,q,s\right) &= -\log\left(1+\frac{1}{\kappa}\right) + \zeta_1\left(\tau\right) - \frac{1}{2}\zeta_2\left(\tau\right)\left(2q+1\right) + se^{-\tau}. \end{aligned} \tag{54}$$

We can see that the value function v becomes independent from s exponentially fast

$$v(\tau, s, q) - C_0\tau \longrightarrow \theta_1 + \mu \cdot q - \frac{\sigma^2}{4}q^2, \quad \tau \longrightarrow \infty, \tag{55}$$

where

$$\begin{aligned} C_0 &= \frac{2\kappa A}{(\kappa+1)}\left(\frac{1}{\kappa} - \log\left(1+\frac{1}{\kappa}\right)\right) - \frac{\sigma^2\kappa A}{(\kappa+1)}, \\ \theta_1 &= \frac{\sigma^2\kappa A}{(\kappa+1)}. \end{aligned} \tag{56}$$

The optimal prices converge to the following limits.

$$\begin{aligned} p_\infty^{a*}(q) &= \log\left(1+\frac{1}{\kappa}\right) + \mu - \frac{\sigma^2}{4}(2q-1) \\ p_\infty^{b*}(q) &= -\log\left(1+\frac{1}{\kappa}\right) + \mu - \frac{\sigma^2}{4}(2q+1), \end{aligned} \tag{57}$$

where the slope with respect to q relies only on the scaled σ. In order for the linearization in (48) to work well, the terms $\kappa\delta^{a*}$ and $\kappa\delta^{b*}$ are required to be small. According to (57), the terms δ^{a*} and δ^{b*} will be linear with respect to q when time is far away from terminal, so at least in this time regime, Zhang's small κ analysis is only valid for sufficiently small q.

We compare the optimal feedback ask limit prices computed by our numerical methods to those in the limit of Zhang's approximation[2] in Figure 1. We plot the feedback ask limit prices as functions of inventory q as they have already become insensitive to the reference price s. Translation is applied on those feedback optimal prices to make them comparable. If we focus on a single model, with small κ or medium κ, we can see that soon after (backwards in time) the ask prices become insensitive to the reference price, the optimal prices (the blue dots for medium κ and the red ones for small κ) are close to the limit of the optimal prices in Zhang's approximation (the black line). On the other hand, after a long time (again backwards in time), the optimal prices (the green dots for medium κ and the yellow line for small κ) become much less sensitive to the inventory q as well and very different from the result in Zhang's approximation. When comparing prices from models with different parameters, we see that even though eventually all those feedback prices would become "flat," it takes much longer for the feedback prices corresponding to small κ to become insensitive to q than for those corresponding to medium κ. The reason that Zhang's small κ approximation works well even for medium κ near the terminal time is that we use small σ in this case, which results in the optimal spreads δ^{a*} and δ^{b*} being relatively small.

4.3. Model with linear utility. When time is far away from the terminal time, the trader has little pressure from risk aversion rooted in the terminal exponential utility, so we expect the trading pattern in such a scenario to be similar to the one in the model with linear utility

$$E\left(X_T + Q_T S_T\right), \tag{58}$$

[2]The shared parameters are $A = 10$ and $\sigma = 0.02$. We considered one model with medium κ ($\kappa = 6$) and another one with small κ ($\kappa = 1$).

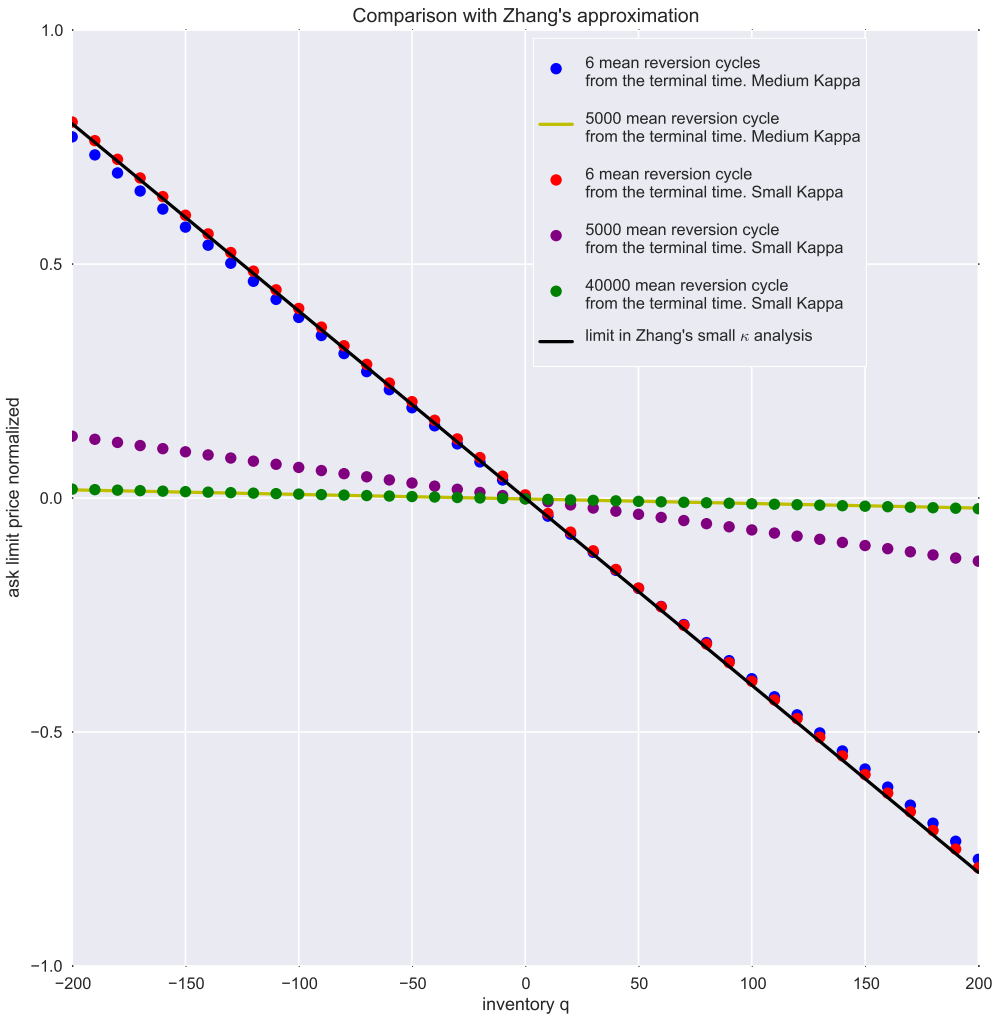

Figure 1. *We plot optimal ask limit order prices at different times from the model with small κ ($\kappa = 1$) and the model with medium κ ($\kappa = 6$). The black line is the ask price in Zhang's small κ analysis for comparison. The prices here are observable prices in the market before the price-scaling described in section 2.3 instead of dimensionless prices after the price-scaling. To make the prices from different models comparable, we subtract the optimal feedback ask price at $q = 0$ from each feedback ask price function. Note that after this normalization, the limit of Zhang's small κ approximation from two models coincides with each other.*
When time is sufficiently far away from the terminal time, the optimal ask limit order prices from both models become significantly different from the limit in Zhang's small κ analysis and converge a constant. Moreover, the limit order price in the model with small κ tends to a constant more slowly than the one in the model with medium κ.

which can be view as a degenerate case of the model with the exponential utility when $\gamma \longrightarrow 0$.

In [19], Fodra and Labadie have considered this case and have obtained the analytical solution for the optimal prices:

$$\hat{p}^{a*}(t,s) = \frac{1}{\kappa} + E_{t,s}(S_T), \quad \hat{p}^{b*}(t,s) = -\frac{1}{\kappa} + E_{t,s}(S_T), \tag{59}$$

where for the OU process

$$E_{t,s}(S_T) = s \cdot e^{-(T-t)} + \mu \cdot \left(1 - e^{-(T-t)}\right) \longrightarrow \mu \quad (T - t \longrightarrow \infty) \tag{60}$$

Thus, in the linear utility model, the optimal feedback limit order prices would converge exponentially fast to

$$\hat{p}^{a*}_{\infty} = \mu + \frac{1}{\kappa}, \quad \hat{p}^{b*}_{\infty} = \mu - \frac{1}{\kappa} \tag{61}$$

Recall that the limits of the dimensionless optimal feedback prices in our model with exponential utility are

$$p^{a*}_{\infty} = \mu + \log\left(1 + \frac{1}{\kappa}\right); \quad p^{b*}_{\infty} = \mu - \log\left(1 + \frac{1}{\kappa}\right). \tag{62}$$

If we do not do price-scaling, namely we do not scale every price-related quantity by γ, then the limit of the optimal prices, which are dimensional in this case, are

$$p^{a*}_{\infty} = \mu + \frac{1}{\gamma}\log\left(1 + \frac{\gamma}{\kappa}\right), \quad p^{b*}_{\infty} = \mu - \frac{1}{\gamma}\log\left(1 + \frac{\gamma}{\kappa}\right) \tag{63}$$

Note that $\frac{1}{\kappa}$ in (61) is just the limit of $\frac{1}{\gamma}\log\left(1 + \frac{\gamma}{\kappa}\right)$ in (63) when the risk aversion parameter $\gamma \longrightarrow 0$, so the limits denied from those two models are consistent.

In the linear utility case, the constant strategy is almost optimal when $T - t$ becomes greater than several mean reversion cycles of the reference price. Since the linear utility is a degenerate case of the exponential utility, it is not surprising that in the exponential utility case, the strategy with constant limit prices also becomes optimal when $T - t$ is large.

4.4. Analogy to pairs trading. The limiting constant price strategy in our model is analogous to pairs trading, a popular strategy in quantitative trading. See [38] for a review.

In pairs trading, a trader opens a long-short position when the relative price, namely the difference between the target pair of assets, deviates from or gets close to its long term mean. More specifically, the trader will set constant levels for relative price at $\hat{\mu} \pm M\hat{\sigma}$ for building up his/her position and the ones at $\hat{\mu} \pm m\hat{\sigma}$ for clearing the position, where $\hat{\mu}$ and $\hat{\sigma}$ are the long term mean and standard deviation of the relative price and $M > m$. In other words, in pairs trading, the trader trades at "constant" levels when considering the mean-reverting relative price.

One difference between our model and pairs trading is that the trader in pairs trading submits market orders, not limit orders. Limit order traders have less control over the inventory if they set their limit prices as constants, which could be an issue especially when we take risk aversion into account. So it is reasonable for limit order traders to update their limit order prices according to their inventory as time approaches the terminal one.

5. Numerical results. We apply the numerical methods described in Section 3 to solve the HJB equation (28) for the value function and optimal controls in our model.

5.1. Evolution of optimal feedback limit order prices. We are interested in how the optimal feedback controls in our model, namely the optimal limit order prices, evolve as a function of the inventory and reference price. As stated in section 4, we observe that the optimal prices converge to constants in (39) when time is away from terminal. In addition, as shown in Figure 2, we observe that the optimal limit order prices become insensitive to the reference price much faster than to the inventory. So between the near-terminal-time regime, where the trader would track the reference price closely, and the away-from-terminal-time regime, where the optimal limit order prices are effectively constants, there is an "intermediate" time regime where the optimal limit order prices only respond to the change of inventory.

For a model with unscaled parameters $A = 10$, $\sigma = 0.05$, $\gamma = 0.005$, $\kappa = 5.0$, $\mu = 1$ and $\alpha = 1$, Figure 2 shows the optimal feedback ask prices at

1. the terminal time,
2. 1 mean reversion cycle of the reference price from the terminal time,
3. 4 mean reversion cycles from the terminal time
4. 800 mean reversion cycles from the terminal time.

Instead of making a 3D plot for the optimal ask price as a function of both the reference price and the inventory, we plot the optimal ask price as a function of only the reference price while each curve in the plot corresponds to a value of the inventory[3].

In the third plot, the optimal prices have become insensitive to the reference price. However, it takes 800 mean reversion cycles to observe the same phenomenon occurs to the inventory, as shown in the bottom plot in Figure 2. This indicates that, with the inventory fixed, the optimal feedback prices are approaching the limits in the equation (39) very slowly.

Note that such difference in the convergence rate occurs across all the numerical experiments we have done with various groups of parameters. In practice, given limited life-time for the mean reversion feature of the asset price, we might only see the insensitivity of optimal limit prices to the reference price, but not to the inventory. Therefore, for a large portion of a trading period, the trader would post limit orders with prices only affected by the change of his own inventory ignoring the fluctuation of the reference price. We call such time regime "intermediate regime" and it can be observed in the simulation results in Section 5.2.

5.2. Simulation results. We show some simulation results of our trading models in Figure 3 and Figure 4. The unscaled parameters used in Figure 3 are $A = 2$, $\sigma = 0.4$, $\gamma = 2$, $\kappa = 1.5$, $\mu = 1$ and $\alpha = 1$; the ones used in Figure 4 are the same except that $A = 6$. We choose those parameters so that the intermediate regime can be observed more clearly. For instance, we choose a large γ so that a jump of the optimal prices due to a change in inventory is evident.

Figure 3 shows a simulation result for 10 mean reversion cycles of reference price. Between time 0 and 8, the trading is in the intermediate regime in the sense that the optimal limit order prices will remain almost constant when no limit order is taken and will jump when the inventory changes. Note that the intermediate regime corresponds to the third plot from

[3]The values for inventory are $\{-750, -600, -450, \cdots, 600, 750\}$.

top in Figure 2, and the jump size here is related to the size of the margin between each flat line in that plot. As shown in the bottom plot in Figure 2, such a margin would go to 0 when time is sufficiently far away from terminal, which means the optimal limit order prices would eventually become constants and the model moves from the intermediate regime to the far-away-from-terminal regime. However it takes much longer to reach that regime and, thus, it is not shown in Figure 3

In Figure 4, the model has the same parameters except that A is greater. Recall that A represents the volume of incoming market orders. So with greater A, more limit orders would be taken. This is evident when comparing the middle plots in Figure 3 and Figure 4. In the top plot of Figure 4, it seems that the optimal prices are tracking the reference price. However a closer look shows that the pattern in this plot is essentially the same as the pattern in the top plot of Figure 3. That is, the limit order prices effectively respond oly to the change of inventory and ignore the fluctuation of the reference price, which suggests that we are in the "intermediate regime." For instance, between time 2 and 3 in the top plot of Figure 4, there is a significant drop of the reference price, but the limit prices does not drop accordingly. They start to decrease only after the inventory increases. In this case, parameter A is sufficiently large that enough limit orders will be taken in one trend of price, which builds up a trend in the inventory and in turn creates a trend in the optimal limit order prices. This explains why on first sight, the limit order prices follow the same trend as the reference price, and why there is a lag between the trend of the reference price and that of the limit order prices.

Note that, when dealing with the mean-reverting reference price, and as long as the time is sufficiently far from terminal, the trader would buy low and sell high focusing on the long term mean of the reference price instead of tracking the reference price closely. This explains why the optimal spreads could possibly go negative as shown, for example, in Figure 3 and Figure 4. This could happen particularly when the time is far away from terminal and the reference price deviates significantly from its long term mean.

When the model moves from the near-terminal regime to the intermediate regime, the sensitivity of the optimal prices to the inventory is mainly affected by the scaled σ. We observed that the greater the scaled σ is, the greater the jump size of the optimal prices is when the inventory changes by one unit. The magnitude of a jump decays to 0 as time goes backwards, with the decay rate affected by A and κ; for greater values of A and κ, the jump size decays faster. Note that, larger values of A and κ means a larger market order flow and a shallower order book respectively. These properties signify higher liquidity in the market. So one insight we can gain from this model is that, for a limit order trader trading a liquid asset with mean-reverting price, his optimal limit prices converge faster backwards in time then they do in the case where he trades a less liquid asset, and therefore his optimal limit prices are less sensitive to the change of inventory.

Recall that here the parameters are the ones after scalings described in section 2.3, so A, κ, and σ^2 are in fact $\frac{A}{\alpha}$, $\frac{\kappa}{\gamma}$, and $\frac{\gamma^2\sigma^2}{\alpha}$ in terms of the parameters before scalings. In contrast, the prices in the figures shown in this section are those before the price-scaling described in section 2.3. That is, they are the observable prices instead of the dimensionless ones.

6. Equilibrium analysis. To check whether our numerical solution of the system in (28) is still valid even when time is far away from terminal, we analytically consider below the

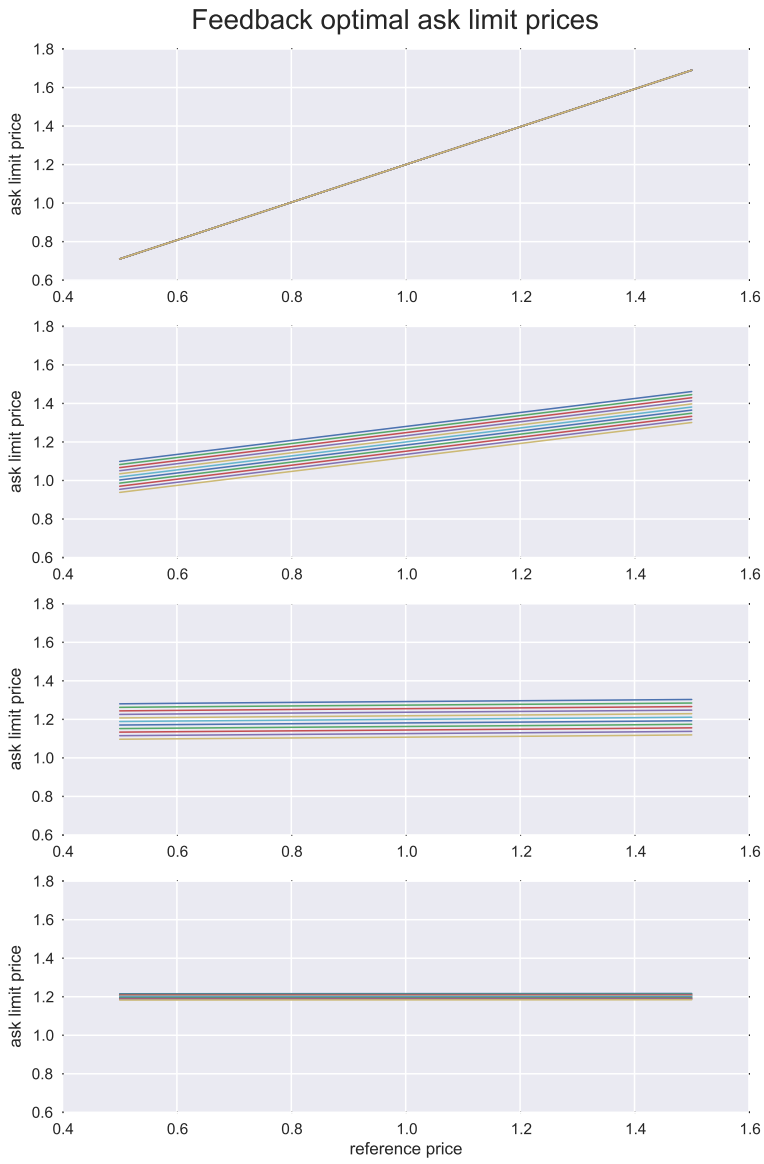

Figure 2. *Feedback optimal ask limit order prices, from top to bottom, corresponding to 0, 1, 4 and 800 mean reversion cycles from the terminal time. The prices are the ones before the price-scaling described in section 2.3 instead of the dimensionless ones after the scaling. Each line, as a function of reference price, corresponds to a value of inventory. The optimal ask prices have already become independent from the reference price at 4 mean reversion cycles from the terminal time (the 3rd plot from top), while it took 800 mean reversion cycles (backwards in time) to become independent from the inventory as well (the bottom plot). Here the 3rd plot from top corresponds to the intermediate regime and the bottom plot corresponds to the far-away-from-terminal regime.*

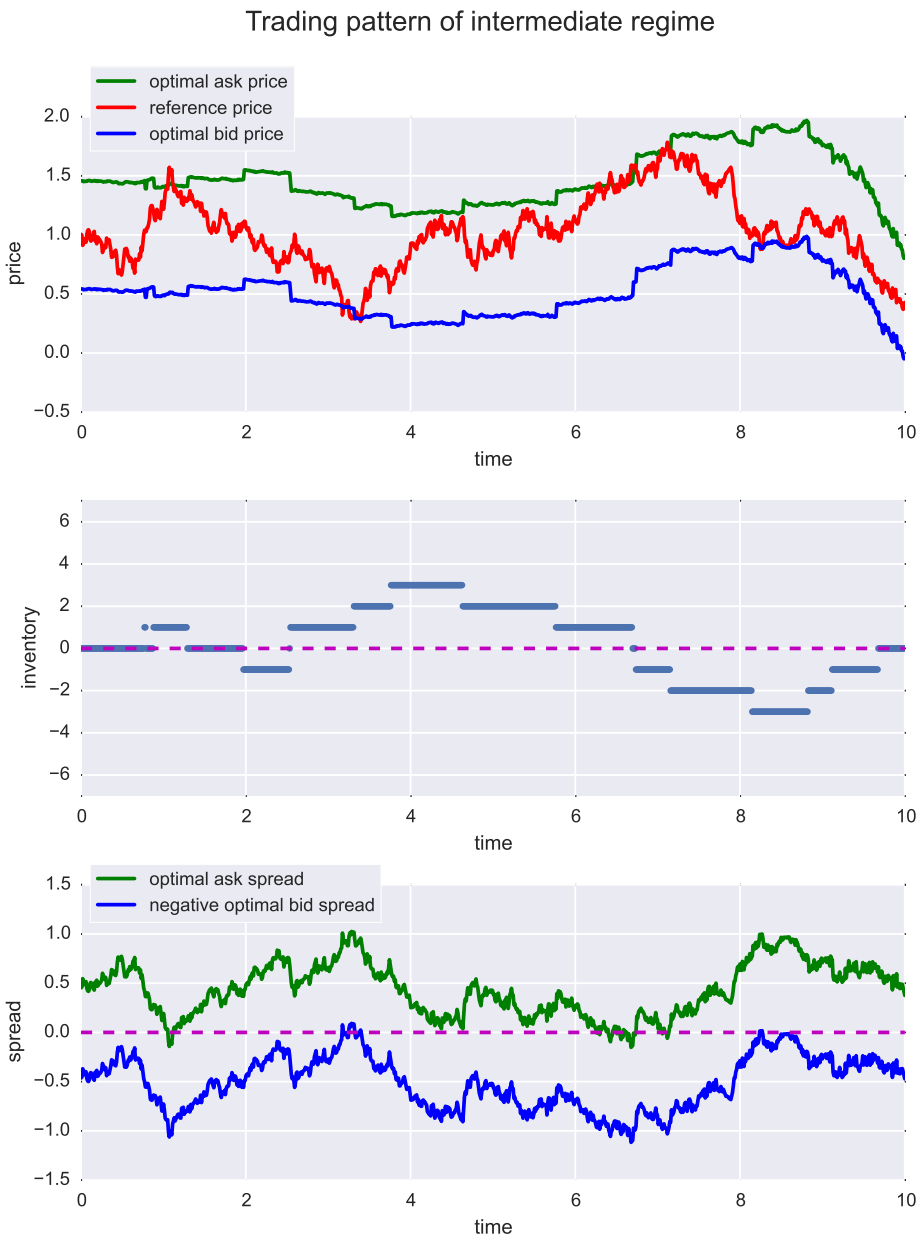

Figure 3. *Simulation results for limit order prices, inventory, and spreads for 10 mean reversion cycles of the underlying reference price. The pattern clearly shows that near the terminal time, the trader tracks the reference price closely whereas in the intermediate regime, the optimal limit prices effectively only respond to the change of inventory.*

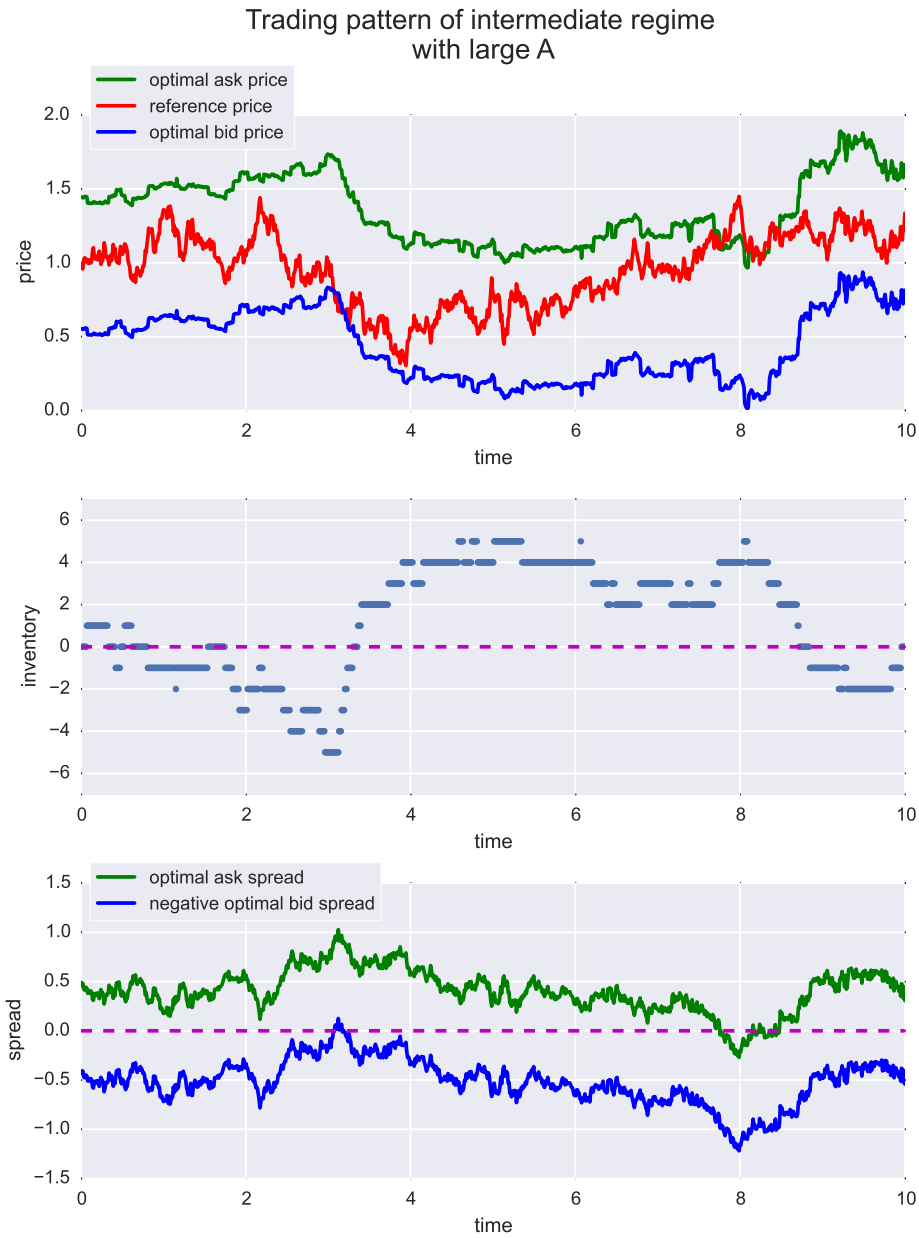

Figure 4. *Similar plots to Figure 3, but with larger parameter A representing greater volume of incoming market orders. When there is a trend in the reference price, for instance, between time 2 and 4, there will also be a trend in optimal prices in the same direction but with a lag. The trend in optimal prices is a result of the trend in the inventory formed during a trend of the reference price when the volume of incoming market orders is large.*

equilibrium of that system and compare the result with our numerical solution of the time-dependent system.

As described in Section 4, our conjecture is that, for a solution v of the PDE (28) and any q and s,

$$v(\tau, q, s) - v(\tau, q-1, s) \longrightarrow \mu \quad (\tau \longrightarrow \infty). \tag{64}$$

Thus, for the equilibrium, we expect

$$v(\tau, q, s) - C\tau \longrightarrow \theta_0 + \theta(s) + \mu q \quad (\tau \longrightarrow \infty) \tag{65}$$

where θ_0 is a constant and $\theta(s)$ satisfies the equilibrium HJB Equation

$$\begin{cases} 0 = C + \frac{\sigma^2}{2}\left(\theta_s^2 - \theta_{ss}\right) - (\mu - s)\,\theta_s - M\left[e^{-\kappa(-s+\mu)} + e^{-\kappa(s-\mu)}\right] \\ \theta(\mu) = 0 \end{cases} \tag{66}$$

with $M = \frac{A}{\kappa+1}\left(1 + \frac{1}{\kappa}\right)^{-\kappa} > 0$. Therefore, when τ is large, we expect the "s-dependent" part of v, defined as $v(\tau, q, s) - v(\tau, q, \mu)$, to be close to $\theta(s)$, the solution to (66). We will transform (66) to a Schrödinger eigenvalue problem, then solve it and compare the result to the numerical solution of v when time is away from terminal.

Moreover, recall that Zhang [52] has obtained a closed form solution of the linearized model with small κ. We can compare the limit of a value function in our model in (65), and the one in Zhang's small κ analysis in (55). In both equations, when $\tau = T - t$ is large, the derivative of the value function with respect to τ is a constant: C in (65) and C_0 in (55). We will show in Section 6.4 that,

$$\lim_{\kappa \to 0} C = \lim_{\kappa \to 0} C_0. \tag{67}$$

That is, the constants in two convergence results are consistent when κ is small.

The differences between (65) and (55) are

1. (55) provides an explicit formula for the constant term θ_1 in the limit, while more information is needed to analytically determine θ_0 in (65).
2. The limit in (65) depends on the variable s while the limit in (55) does not. Our numerical simulations, shown in Figure 5, confirm the dependence of the limit of the value function on s. On the other hand, when κ is small, we observe that the value function from our numerical simulation is almost flat with respect to s, which is consistent with (55) and can be viewed as the limit phenomena when κ approaches 0. See Section 6.6 for the simulation result.
3. The limit in (55) has a quadratic term of q, which leads to a linear term of q with fixed non-zero coefficient in the limit of optimal prices. However, our numerical simulation shows that given sufficiently long time, the optimal prices will become flat with respect to q instead of growing linearly.

Note that the limit in (65) is indeed a solution of the HJB equation in (28), but it does not satisfy the initial condition. Now we analyze equation (66) to gain some insight into constant C and solution θ.

6.1. Riccati equation for the equilibrium value function. Let $l = \theta_s$, which satisfies the following Riccati equation

$$l' = l^2 - \frac{2}{\sigma^2}(\mu - s)\, l + \frac{2C}{\sigma^2} - \frac{2M}{\sigma^2}\left[e^{-\kappa(-s+\mu)} + e^{-\kappa(s-\mu)}\right] \tag{68}$$

Here, we could assume $\mu = 0$, or equivalently we can make a change of variable $s - \mu \longrightarrow s$ so that

$$l' = l^2 + \frac{2}{\sigma^2} s \cdot l + \frac{2C}{\sigma^2} - \frac{2M}{\sigma^2}\left[e^{\kappa s} + e^{-\kappa s}\right] \tag{69}$$

6.2. Sturm-Liouville eigenvalue problem. We can apply the transformation

$$l = -\frac{m'}{m} \tag{70}$$

to transform the (69) to a second order linear equation:

$$m'' - \frac{2}{\sigma^2} s \cdot m' - \frac{2M}{\sigma^2}\left[e^{\kappa s} + e^{-\kappa s}\right] \cdot m + C \cdot \frac{2}{\sigma^2} \cdot m = 0. \tag{71}$$

This can be written in the form

$$-\left(e^{-\frac{1}{\sigma^2}s^2} \cdot m'\right)' + e^{-\frac{1}{\sigma^2}s^2} \cdot \frac{2M}{\sigma^2}\left[e^{\kappa s} + e^{-\kappa s}\right] \cdot m = C \cdot \frac{2}{\sigma^2} e^{-\frac{1}{\sigma^2}s^2} \cdot m \tag{72}$$

and viewed as the Sturm-Liouville eigenvalue problem of the operator

$$L[m] = -\left(e^{-\frac{1}{\sigma^2}s^2} \cdot m'\right)' + e^{-\frac{1}{\sigma^2}s^2} \cdot \frac{2M}{\sigma^2}\left[e^{\kappa s} + e^{-\kappa s}\right] \cdot m \tag{73}$$

The spectrum of such a Sturm-Liouville problem is discrete, and the proof can be found in [7]. We are looking for the smallest eigenvalue in the eigenvalue problem and the corresponding eigenfunction which vanishes at infinity and does not change its sign.

Note that the theoretical properties of the eigenfunction match our expectation on θ from the numerical simulation of the limit of v in (28).

1. The eigenfunction m does not have any root, so function $l = -\frac{m'}{m}$ and, in turn, θ are defined globally.
2. From (70), we have $m(s) = m_0 \cdot e^{-(\theta(s)-\theta(0))}$, so if it vanishes at $\pm\infty$, then θ would go to $+\infty$ when s goes to $\pm\infty$. This is consistent with our numerical simulation for (28), in which we observed that, when τ is large, the function $v(\tau, q, s)$ goes to ∞ when s goes to $\pm\infty$.

6.3. Shrodinger equation. We could also consider

$$\hat{m} = e^{-\frac{1}{2\sigma^2}s^2} m \tag{74}$$

which satisfies

$$-\hat{m}'' + \left[\frac{s^2}{\sigma^4} + \frac{2M}{\sigma^2}\left(e^{\kappa s} + e^{-\kappa s}\right)\right] \cdot \hat{m} = \hat{C} \cdot \hat{m} \tag{75}$$

where $\hat{C} = C\frac{2}{\sigma^2} + \frac{1}{\sigma^2}$. Here we have a Schrödinger operator

$$\hat{L}\left[\hat{m}\right] = -\hat{m}'' + \left[\frac{s^2}{\sigma^4} + \frac{2M}{\sigma^2}\left(e^{\kappa s} + e^{-\kappa s}\right)\right] \cdot \hat{m} \tag{76}$$

with an unbounded positive potential. Therefore, it has a lower-bounded discrete spectrum (see Theorem 7.3 in [44] for instance). Again, we are looking for the smallest eigenvalue whose eigenfunction vanishes at infinity and does not change its sign on the real line.

6.4. Small κ expansion on the Schrödinger operator. As mentioned at the beginning of this section, we will show that the constant C in (65) is consistent with C_0 in (55) when κ goes to 0.

For κ small, we expand the exponential terms in (75) as

$$e^{\kappa s} + e^{-\kappa s} \approx 2 + \kappa^2 s^2 \tag{77}$$

which reduces (75) to

$$-\hat{m}'' + \left(\frac{1}{\sigma^4} + \frac{2\kappa^2 M}{\sigma^2}\right) s^2 \cdot \hat{m} = (\hat{C} - \frac{4M}{\sigma^2})\hat{m} \tag{78}$$

The corresponding eigenvalue problem is explicitly solvable since the potential here is a quadratic function of s. Applying the formula for the smallest eigenvalue of the harmonic oscillator, we have

$$\hat{C} - \frac{4M}{\sigma^2} = \sqrt{\frac{1}{\sigma^4} + \frac{2\kappa^2 M}{\sigma^2}}. \tag{79}$$

Since $\hat{C}$ is defined by $\hat{C} = C\frac{2}{\sigma^2} + \frac{1}{\sigma^2}$, we have

$$C = -\frac{1}{2} + 2M + \frac{1}{2}\sqrt{1 + 2\kappa^2 M\sigma^2}. \tag{80}$$

Recall that $M = \frac{A}{\kappa+1}\left(1 + \frac{1}{\kappa}\right)^{-\kappa}$ and $C_0 = \frac{2\kappa A}{(\kappa+1)}\left(\frac{1}{\kappa} - \log\left(1 + \frac{1}{\kappa}\right)\right) - \frac{\sigma^2\kappa A}{(\kappa+1)}$. So

$$\begin{aligned} &\lim_{\kappa\to 0} M = A \\ &\lim_{\kappa\to 0} C_0 = 2A \\ \Longrightarrow &\lim_{\kappa\to 0} C = 2A = \lim_{\kappa\to 0} C_0 \end{aligned} \tag{81}$$

6.5. The smallest eigenvalue of the Schrödinger operator. Here we heuristically discuss how the smallest eigenvalue of the Schrödinger operator in equation (76) appears in the limit of v in (28).

When τ is large, both terms $v\left(\tau, q, s\right) - v\left(\tau, q-1, s\right)$ and $v\left(\tau, q+1, s\right) - v\left(\tau, q, s\right)$ in (28) are close to μ, so we replace those two terms by μ in our heuristic derivation. Moreover, we

make a change of variable $s-\mu \longrightarrow s$ for simplification which transforms (28) to the following equation

$$0 = v_\tau + \frac{\sigma^2}{2}\left(v_s^2 - v_{ss}\right) + s v_s - \frac{A}{\kappa+1}\left(1+\frac{1}{\kappa}\right)^{-\kappa}\left(e^{\kappa s} + e^{-\kappa s}\right). \tag{82}$$

Note that q does appear explicitly in (82). Therefore, we can treat v in equation (82) as a function of just τ and s and view q as a parameter.

We now show that the limit of v_τ in (82) is closely related to the smallest eigenvalue of the operator in (76). Consider $\hat{v} = e^{-v-\frac{1}{2\sigma^2}s^2}$ which satisfies

$$-\hat{v}_\tau = \frac{\sigma^2}{2}\left[-\hat{v}_{ss} + \left(\frac{s^2}{\sigma^4} + \frac{2M}{\sigma^2}\left(e^{\kappa s} + e^{-\kappa s}\right) - \frac{1}{\sigma^2}\right)\hat{v}\right] \tag{83}$$

The operator

$$L_s\left[\hat{v}\right] = \frac{\sigma^2}{2}\left[-\hat{v}_{ss} + \left(\frac{s^2}{\sigma^4} + \frac{2M}{\sigma^2}\left(e^{\kappa s} + e^{-\kappa s}\right) - \frac{1}{\sigma^2}\right)\hat{v}\right] \tag{84}$$

can be viewed as the Schrödinger operator in equation (76) being slightly modified, and the sets of eigenvalues of those two operators have an order-preserving 1-1 correspondence. It still has lower-bounded discrete specturm. Assume that its eigenvalues are $\lambda_1 \le \lambda_2 \le \cdots$ and the corresponding orthonormal eigenbasis is given by $\{f_1, f_2, \cdots\}$. The solution of equation (83) can be written as

$$\hat{v}\left(\tau, s\right) = \sum_{n\ge 1} a_n\left(\tau\right) f_n\left(s\right) \tag{85}$$

and

$$a_n'\left(\tau\right) = -\lambda_n a_n\left(\tau\right) \Longrightarrow a_n\left(\tau\right) = k_n e^{-\lambda_n \tau} \tag{86}$$

As a result, it follows that

$$\begin{aligned} -v_\tau = \frac{\hat{v}_\tau}{\hat{v}} &= \frac{\sum_{n\ge 1} -\lambda_n k_n e^{-\lambda_n \tau} f_n\left(s\right)}{\sum_{n\ge 1} k_n e^{-\lambda_n \tau} f_n\left(s\right)} \\ &= \frac{-\lambda_1 k_1 f_1 + \sum_{n\ge 2} -\lambda_n k_n e^{-(\lambda_n-\lambda_1)\tau} f_n\left(s\right)}{k_1 f_1 + \sum_{n\ge 2} k_n e^{-(\lambda_n-\lambda_1)\tau} f_n\left(s\right)} \\ &\longrightarrow -\lambda_1 \quad (\tau \longrightarrow \infty) \end{aligned} \tag{87}$$

So formally, v_τ would converge to λ_1, the smallest eigenvalue of the operator in the equation (84), which also directly corresponds to the smallest eigenvalue of the operator in equation (76).

6.6. Numerical results on the equilibrium equation. We would like to solve the equation (71) to find the constant C that yield a solution which vanishes at infinity and does not change its sign. Because of the convergence in the equation (65), v_τ with large τ could serve as an estimate of the constant C. We search around such estimate to find the desired constant C. After we get the constant C, we compute the solution of the following system, which is derived from (71),

$$\begin{cases} m' = n \\ n' = \frac{2}{\sigma^2} s \cdot n + \frac{2}{\sigma^2} \left[M \left(e^{\kappa s} + e^{-\kappa s} \right) - C \right] \cdot m. \end{cases} \tag{88}$$

We need to specify the initial conditions $m(0)$ and $n(0)$. Since equation (71) is homogeneous, $m(0)$ could be arbitrary, so we set $m(0) = 1$ for simplicity. Additionally, we set $n(0) = 0$ due to the symmetry of the equation. As a result, the data is

$$\begin{cases} m(0) = 1 \\ n(0) = 0 \end{cases} \tag{89}$$

Consider two models with shared parameters

$$A = 0.9, \quad \sigma = 0.3, \quad \gamma = 0.01, \quad \mu = 1.0 \tag{90}$$

and different values of κ:

$$\kappa = \begin{cases} 0.3 & \text{in the first model,} \\ 0.01 & \text{in the second model} \end{cases} \tag{91}$$

where the parameters are the ones before the price-scaling.

We numerically solve (88) for $m(s)$, then in turn compute $\theta(s)$ with $\theta(\mu) = 0$ in (66). We compare it in Figure 5 to the "s-dependent" part of v which is defined as

$$v_{Limit}(s) - v_{Limit}(\mu) \tag{92}$$

where $v_{Limit}(s) \triangleq v(\tau, q = 0, s)$ for large τ. We can see that for each model, $\theta(s)$ is very close to the "s-dependent" part of v, and that for the model with smaller κ, $\theta(s)$ is flatter. Note that the result in section 4.2, which states that the limits of v calculated via a small κ expansion does not depend on s, can be viewed as the limit when κ goes to 0.

6.7. Bounds of the smallest eigenvalue of the Schrödinger operator. The Rayleigh Quotient provides a way to express the smallest eigenvalue of the Schrödinger operator in (75):

$$c_0 = \inf_{u \neq 0} \frac{\int_{\mathbb{R}} (u')^2 + \int_{\mathbb{R}} v \cdot u^2}{\int_{\mathbb{R}} u^2} \tag{93}$$

where $v = \frac{s^2}{\sigma^4} + \frac{2M}{\sigma^2} \left(e^{\kappa s} + e^{-\kappa s} \right)$ is the potential.

By plugging an arbitrary function in the function space to the quotient, we can obtain an upper bound of the smallest eigenvalue. To find a lower bound, we find a solvable problem with potential $\tilde{v}$ where $\tilde{v} \leq v$ which yields $\tilde{c}_0 \leq c_0$.

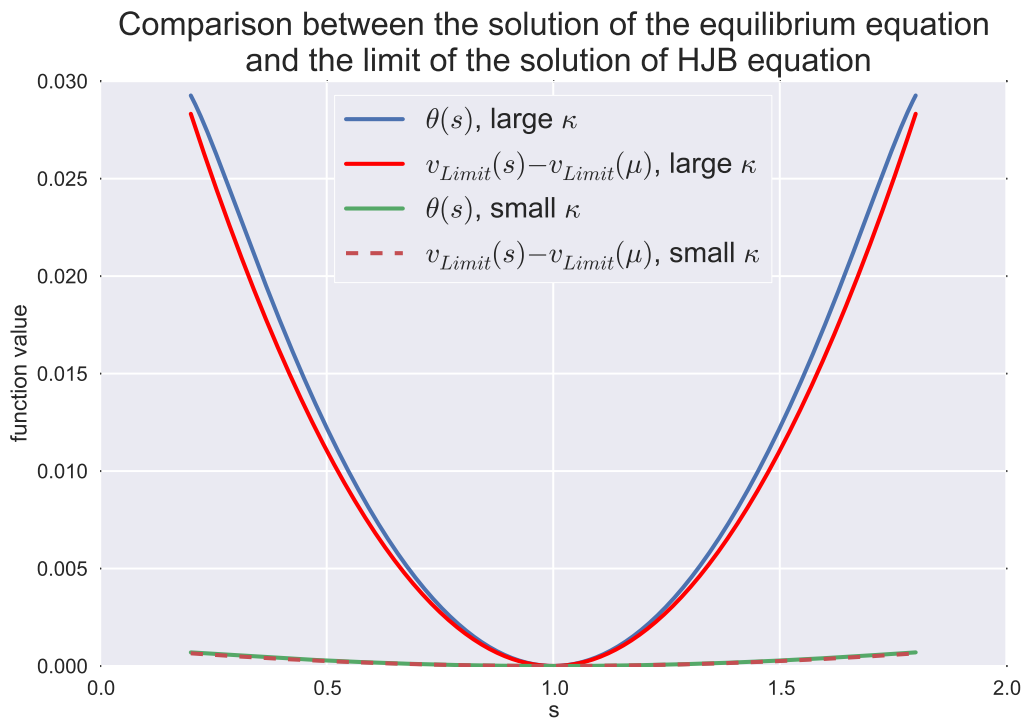

Figure 5. *We compare $\theta(s)$ in the Schrödinger equation (66) and $v_{Limit}(s) - v_{Limit}(\mu)$, namely the "s-dependent" part of the function v from the numerical result of the time dependent system in equation (28) when time is far away from terminal. Here $\theta(s)$ and $v_{Limit}(s) - v_{Limit}(\mu)$ match very well for both large κ ($\kappa = 0.3$) and the small κ ($\kappa = 0.01$). When κ is small, both $\theta(s)$ and $v_{Limit}(s) - v_{Limit}(\mu)$ are flat, which is consistent with the result in Zhang's small κ analysis.*

6.7.1. Upper bound. To obtain an upper bound, we minimize the Rayleigh quotient with respect to the set of Gaussian kernels

$$u(s) = e^{-\frac{(s-p_2)^2}{p_1^2}} \tag{94}$$

with parameters p_1 and p_2. Plugging in the Gaussian kernel to the quotient, we have

$$\frac{\int_{\mathbb{R}} (u')^2 + \int_{\mathbb{R}} v \cdot u^2}{\int_{\mathbb{R}} u^2} = \frac{1}{p_1^2} + \frac{1}{4\sigma^4} p_1^2 + \frac{1}{\sigma^4} p_2^2 + \frac{2M}{\sigma^2} \left[e^{-\kappa p_2} + e^{\kappa p_2} \right] e^{\frac{1}{8}\kappa^2 p_1^2} \tag{95}$$

To minimize the expression, p_2 should be 0, and p_1^2 should minimize

$$f(x) = \frac{1}{x} + \frac{1}{4\sigma^4} x + \frac{4M}{\sigma^2} e^{\frac{1}{8}\kappa^2 x}, \quad x > 0 \tag{96}$$

where

$$\begin{aligned} f' &= -\frac{1}{x^2} + \frac{1}{4\sigma^4} + \frac{4M}{\sigma^2} \frac{1}{8} \kappa^2 \cdot e^{\frac{1}{8}\kappa^2 x} \\ f'' &= \frac{2}{x^3} + \frac{4M}{\sigma^2} \left(\frac{1}{8} \kappa^2 \right)^2 \cdot e^{\frac{1}{8}\kappa^2 x} > 0 \text{ for } x > 0 \end{aligned} \tag{97}$$

Since $f'(0+) = -\infty$ and $f'(+\infty) = +\infty$, f' has a unique root x_0 which can be computed numerically. This yields the minimum point of f as desired. It turns out that $f(x_0)$ gives a reasonably good approximation of the eigenvalue.

We try the following two sets of the parameters, in which cases the upper bound for C is very close to our numerical result.

(1) $A = 2.5$, $\kappa = 1.5$, $\sigma = \frac{3}{\sqrt{10}}$.
In this case, $\left(f(x_0) - \frac{1}{\sigma^2}\right) \cdot \frac{\sigma^2}{2} = 1.3197$ gives an upper bound of the constant C, while the value of C obtained from the method described in section 6.6 is 1.3191.

(2) $A = 10$, $\kappa = 1.5$, $\sigma = \frac{3}{\sqrt{10}}$.
In this case, $\left(f(x_0) - \frac{1}{\sigma^2}\right) \cdot \frac{\sigma^2}{2} = 4.7331$, again, gives an upper bound of the constant C, while the value of C obtained numerically is 4.7325.

6.7.2. Lower bound. It is shown in [48] that the operator (with parameter ξ)

$$\mathcal{L}[\psi] = -\psi'' + \left[\frac{1}{8}\xi^2 \cosh(4x) - \frac{2}{\cosh(x)}\right]\psi \tag{98}$$

has the smallest eigenvalue

$$\frac{1}{8}\xi^2 + \xi - 1 \tag{99}$$

and a corresponding eigenfunction

$$\frac{e^{-\frac{1}{4}\xi\cosh(2x)}}{\cosh(x)}. \tag{100}$$

By a change of variable ($\kappa s = 4x$), equation (75) can be rewritten as

$$-\hat{m}'' + \frac{16}{\kappa^2}\left[\frac{\left(\frac{4x}{\kappa}\right)^2}{\sigma^4} + \frac{4M}{\sigma^2}\cosh(4x)\right] \cdot \hat{m} = \frac{16}{\kappa^2}\hat{C} \cdot \hat{m}. \tag{101}$$

By setting

$$\begin{aligned} \frac{1}{8}\xi^2 &= \frac{16}{\kappa^2}\frac{4M}{\sigma^2} \\ \Longrightarrow \xi &= \frac{16\sqrt{2M}}{\kappa\sigma} \end{aligned} \tag{102}$$

in (98), we can compute the smallest eigenvalue $\tilde{c}_0$ of the operator

$$\hat{\mathcal{L}}[\tilde{m}] = -\tilde{m}'' + \left[-\frac{2}{\cosh(x)} + \frac{16}{\kappa^2}\frac{4M}{\sigma^2}\cosh(4x)\right] \cdot \tilde{m} \tag{103}$$

which we will compare to the operator on the left hand side of equation (101). Using (98) and (99), we have

$$\tilde{c}_0 = \frac{1}{8}\left(\frac{16\sqrt{2M}}{\kappa\sigma}\right)^2 + \frac{16\sqrt{2M}}{\kappa\sigma} - 1 \tag{104}$$

Comparing the potential of the operator

$$\hat{\mathcal{L}}\left[\hat{m}\right] = -\hat{m}'' + \left[\left(\frac{16}{\kappa^2}\right)^2 \frac{1}{\sigma^4}x^2 + \frac{16}{\kappa^2}\frac{4M}{\sigma^2}\cosh\left(4x\right)\right]\cdot\hat{m} \tag{105}$$

in (101) to the one in the (103), its smallest eigenvalue, denoted by $\hat{c}_0$, is greater than $\tilde{c}_0$. As a result, we have

$$\begin{aligned} &\frac{16}{\kappa^2}\left(C\frac{2}{\sigma^2} + \frac{1}{\sigma^2}\right) = \hat{c}_0 \geq \tilde{c}_0 = \frac{1}{8}\left(\frac{16\sqrt{2M}}{\kappa\sigma}\right)^2 + \frac{16\sqrt{2M}}{\kappa\sigma} - 1 \\ \Longrightarrow\quad & C \geq \left\{\frac{\kappa^2}{16}\left[\frac{1}{8}\left(\frac{16\sqrt{2M}}{\kappa\sigma}\right)^2 + \frac{16\sqrt{2M}}{\kappa\sigma} - 1\right] - \frac{1}{\sigma^2}\right\}\frac{\sigma^2}{2} \end{aligned} \tag{106}$$

Note that with a constant $k \geq 1$, we have

$$f\left(x\right) = kx^2 + \frac{2}{\cosh\left(x\right)} \geq 2 \tag{107}$$

Thus, instead of the operator in (98), we can compare the operator in (105) to

$$\mathcal{L}\left[m\right] = -m'' + \left[-\frac{2}{\left(\cosh\left(x\right)\right)} + 2 + \frac{16}{\kappa^2}\frac{4M}{\sigma^2}\cosh\left(4x\right)\right]m \tag{108}$$

when

$$\left(\frac{16}{\kappa^2}\right)^2 \frac{1}{\sigma^4} \geq 1 \tag{109}$$

As a result, instead of the one in (106), we have a better lower bound of C when (109) holds;

$$C \geq \left\{\frac{\kappa^2}{16}\left[\frac{1}{8}\left(\frac{16\sqrt{2M}}{\kappa\sigma}\right)^2 + \frac{16\sqrt{2M}}{\kappa\sigma} + 1\right] - \frac{1}{\sigma^2}\right\}\frac{\sigma^2}{2} \tag{110}$$

We try this bound with the same set of parameters used in the previous subsection.

(1) $A = 2.5$, $\kappa = 1.5$, $\sigma = \frac{3}{\sqrt{10}}$.
In this case, the lower bound of C given in (110) is 1.1788, while the numerical result is 1.3191.

(2) $A = 10$, $\kappa = 1.5$, $\sigma = \frac{3}{\sqrt{10}}$.
In this case, the lower bound of C given in (110) is 4.6533, while the numerical result is 4.7325.

7. Conclusion. In this paper, we consider the limit order book model of Avellaneda and Stoikov [3] with a mean reverting underlying price. Our main result is that when time is far from terminal, it is optimal to post constant limit order prices instead of tracking the underlying price. We use two different numerical methods to solve the HJB equation, and both of them confirm the long-time behavior. This result implies that when the underlying price is mean reverting then, when time is far from terminal, it is optimal to focus on the mean price and ignore the fluctuations around it. This observation, admittedly from a stylized model, confirms what limit order traders might expect.

The numerical results also show that between the time regime where constant limit order prices are optimal and the one close to the terminal time, there is an intermediate time period where limit order prices are influenced by the inventory of outstanding orders. The duration of this intermediate period depends on the parameters A and κ that quantify the liquidity of the market.

We also study the equilibrium of the optimal control problem. The equilibrium of the HJB equation can be transformed to a Schrödinger equation, as an eigenvalue problem. The solution agrees with the long-time limit of our numerical result of the time-dependent model, which confirms the validity and accuracy of our numerical methods, even for long time. When the liquidity parameter κ is small, the numerical solutions also match the analysis in Zhang [52].

Even though the numerical calculations strongly suggest convergence of the optimal limit order prices, the proof remains open and needs further study.

Appendix A. Numerical methods.

A.1. Boundary condition. As in [30, 52], we assume that the total amount of the asset available is Q, which means at the boundary point with $q = Q$, buying is forbidden, and at the boundary point with $q = -Q$, selling is forbidden. Those are the boundary conditions at the artificial boundaries $q = \pm Q$ for the inventory space.

It appears that the numerical boundary condition may affect the solution of the optimal control problem described in section 2 even at the points away from the boundary. Here we discuss the model with constant reference price μ as an example. In section 4.1, we have shown that for the model

$$\begin{cases} Q_t^b \sim \text{Poi}\left(Ae^{-\kappa\delta_t^b}\right) \\ Q_t^a \sim \text{Poi}\left(Ae^{-\kappa\delta_t^a}\right) \\ dQ_t = dQ_t^b - dQ_t^a \\ dX_t = \left(\delta_t^a + S_t\right) dQ_t^a - \left(S_t - \delta_t^b\right) dQ_t^b \\ S_t \equiv \mu \\ Q_0 = q_0, \quad X_0 = x_0 \\ \sup\limits_{\delta^a,\delta^b} E\left[-e^{-(X_T+Q_T\mu)}\right], \end{cases} \tag{111}$$

the optimal prices are

$$
\begin{aligned}
p^{a*} &= \mu + \log\left(1 + \frac{1}{\kappa}\right) \\
p^{b*} &= \mu - \log\left(1 + \frac{1}{\kappa}\right).
\end{aligned} \tag{112}
$$

However, if we add boundary conditions at the boundaries $q = \pm Q$, then the system for v in (44) becomes

$$
\begin{aligned}
& v_t(t,q) - \frac{A}{\kappa+1}\left(e^{-\kappa\delta^{b*}} + e^{-\kappa\delta^{a*}}\right) v(t,q) = 0, \quad -Q < q < Q \\
& v_t(t,s,-Q) - \frac{A}{\kappa+1} e^{-\kappa\delta^{b*}} v(t,-Q) = 0 \\
& v_t(t,s,Q) - \frac{A}{\kappa+1} e^{-\kappa\delta^{a*}} v(t,Q) = 0,
\end{aligned}
$$

and the asymptotic optimal limit bid and ask prices become

$$
\begin{aligned}
p^b_\infty(q) &= \mu - \log\left(1 + \frac{1}{\kappa}\right) + \frac{1}{\kappa}\left[\log\sin\left(\frac{(q+Q+2)\pi}{2Q+2}\right) - \log\sin\left(\frac{(q+Q+1)\pi}{2Q+2}\right)\right] \\
p^a_\infty(q) &= \mu + \log\left(1 + \frac{1}{\kappa}\right) + \frac{1}{\kappa}\left[\log\sin\left(\frac{(q+Q+1)\pi}{2Q+2}\right) - \log\sin\left(\frac{(q+Q)\pi}{2Q+2}\right)\right].
\end{aligned} \tag{113}
$$

These are different from the exact solution of the problem without boundary conditions in (112). Note that for $|q| \ll Q$, such a difference is indeed negligible.

This stylized example shows how the numerical boundary conditions affect the solution. In practice, we would set Q fairly large and only check the value function or the optimal prices for $|q| < \frac{Q}{4}$ for instance. Note that in (113), with q fixed and $Q \to \infty$, p^a and p^b converge to the expression in (112), so in this degenerate model,

$$
\begin{aligned}
\lim_{t\to\infty}\lim_{Q\to\infty} p^b(t,q) &= \lim_{Q\to\infty}\lim_{t\to\infty} p^b(t,q), \\
\lim_{t\to\infty}\lim_{Q\to\infty} p^a(t,q) &= \lim_{Q\to\infty}\lim_{t\to\infty} p^a(t,q).
\end{aligned} \tag{114}
$$

We expect that the same result still holds for non-degenerate models. Thus, in practice, we compute $\lim_{t\to\infty} p^b(t,q)$ and $\lim_{t\to\infty} p^a(t,q)$ for fixed q and large Q to approximate $\lim_{t\to\infty}\lim_{Q\to\infty} p^b(t,q)$ and $\lim_{t\to\infty}\lim_{Q\to\infty} p^a(t,q)$.

A.2. Finite difference method. Due to the non-linearity, we implement an implicit finite difference method to solve (28). We discretize the time space $[0,T]$ and the reference-price space $[\mu - S, \mu + S]$ using step-size $\Delta\tau$ and Δs, and consider

$$
v^n_{q,j} \approx v(n\Delta\tau, q, \mu - S + j\Delta s)
$$

where n is the index of the grid point in the time space, q is the number of asset held, and j is the index of the grid point in the reference-price space.

At each step, we assume that $v_{q,j}^n$ is known and we compute $v_{q,j}^{n+1}$. The terms in equation (28) are replaced by the following terms

$$
\begin{aligned}
v_\tau &\approx \frac{v_{q,j}^{n+1} - v_{q,j}^n}{\Delta\tau} \\
v_s^2 &\approx \left(\frac{v_{q,j+1}^{n+1} - v_{q,j-1}^{n+1}}{2\Delta s}\right)^2 \\
(\mu - s)\, v_s &\approx (\mu - s)\, [\frac{v_{q,j+1}^{n+1} - v_{q,j}^{n+1}}{\Delta s} 1_{\mu>s} + \frac{v_{q,j}^{n+1} - v_{q,j-1}^{n+1}}{\Delta s} 1_{\mu<s}] \\
v_{ss} &\approx \frac{v_{q,j+1}^{n+1} - 2v_{q,j}^{n+1} + v_{q,j-1}^{n+1}}{\Delta s^2}.
\end{aligned}
\tag{115}
$$

The discretized PDE is then given by

$$
\begin{aligned}
0 =& \frac{v_{q,j}^{n+1} - v_{q,j}^n}{\Delta\tau} + \frac{\sigma^2}{2}\left(\left(\frac{v_{q,j+1}^{n+1} - v_{q,j-1}^{n+1}}{2\Delta s}\right)^2 - \frac{v_{q,j+1}^{n+1} - 2v_{q,j}^{n+1} + v_{q,j-1}^{n+1}}{\Delta s^2}\right) \\
&- (\mu - s)\left(\frac{v_{q,j+1}^{n+1} - v_{q,j}^{n+1}}{\Delta s} 1_{\mu>s} + \frac{v_{q,j}^{n+1} - v_{q,j-1}^{n+1}}{\Delta s} 1_{\mu<s}\right) \\
&- \frac{A}{\kappa+1}\left(1 + \frac{1}{\kappa}\right)^{-\kappa}\left(e^{-\kappa\left(-s - v_{q-1,j}^{n+1} + v_{q,j}^{n+1}\right)} + e^{-\kappa\left(s - v_{q+1,j}^{n+1} + v_{q,j}^{n+1}\right)}\right)
\end{aligned}
\tag{116}
$$

which can be simplified to

$$
\begin{aligned}
& v_{q,j}^{n+1}\left[1 + \frac{\Delta\tau}{\Delta s^2}\sigma^2 - (\mu - s)\frac{\Delta\tau}{\Delta s}\left(1_{\mu<s} - 1_{\mu>s}\right)\right] \\
&+ v_{q,j+1}^{n+1}\left(-\frac{\Delta\tau}{2\Delta s^2}\sigma^2 - (\mu - s)\frac{\Delta\tau}{\Delta s} 1_{\mu>s}\right) \\
&+ v_{q,j-1}^{n+1}\left(-\frac{\Delta\tau}{2\Delta s^2}\sigma^2 + (\mu - s)\frac{\Delta\tau}{\Delta s} 1_{\mu<s}\right) \\
&= v_{q,j}^n - \frac{\sigma^2}{2}\frac{\Delta\tau}{4\Delta s^2}\left(v_{q,j+1}^{n+1} - v_{q,j-1}^{n+1}\right)^2 \\
&+ \frac{A\Delta\tau}{\kappa+1}\left(1 + \frac{1}{\kappa}\right)^{-\kappa}\left(e^{-\kappa\left(-s - v_{q-1,j}^{n+1} + v_{q,j}^{n+1}\right)} + e^{-\kappa\left(s - v_{q+1,j}^{n+1} + v_{q,j}^{n+1}\right)}\right).
\end{aligned}
\tag{117}
$$

where s is the value of the j-th grid point in the discretized reference-price space.

We use iteration to solve this non-linear equation for $v_{q,j}^{n+1}$. Denote $v_{q,j}^{n+1,k}$ as the solution of this system in k-th iteration. Then in $(k+1)$-th iteration, we solve the following linear

equation for $v_{q,j}^{n+1,k+1}$;

$$
\begin{aligned}
& v_{q,j}^{n+1,k+1}[1+\frac{\Delta\tau}{\Delta s^2}\sigma^2-(\mu-s)\frac{\Delta\tau}{\Delta s}(1_{\mu<s}-1_{\mu>s})] \\
& +v_{q,j+1}^{n+1,k+1}\left(-\frac{\Delta\tau}{2\Delta s^2}\sigma^2-(\mu-s)\frac{\Delta\tau}{\Delta s}1_{\mu>s}\right) \\
& +v_{q,j-1}^{n+1,k+1}\left(-\frac{\Delta\tau}{2\Delta s^2}\sigma^2+(\mu-s)\frac{\Delta\tau}{\Delta s}1_{\mu<s}\right) \\
& =v_{q,j}^{n}-\frac{\sigma^2}{2}\frac{\Delta\tau}{4\Delta s^2}\left(v_{q,j+1}^{n+1,k}-v_{q,j-1}^{n+1,k}\right)^2 \\
& +\frac{A\Delta\tau}{\kappa+1}\left(1+\frac{1}{\kappa}\right)^{-\kappa}\left(e^{-\kappa\left(-s-v_{q-1,j}^{n+1,k}+v_{q,j}^{n+1,k}\right)}+e^{-\kappa\left(s-v_{q+1,j}^{n+1,k}+v_{q,j}^{n+1,k}\right)}\right)
\end{aligned}
\tag{118}
$$

Here all the $v_{q,j}^{n+1}$ on the right hand side are replaced by $v_{q,j}^{n+1,k}$, the result from the last iteration, and all $v_{q,j}^{n+1}$ on the left hand side are replaced by $v_{q,j}^{n+1,k+1}$, the target in the current iteration. We repeat this procedure until the difference between $v_{q,j}^{n+1,k+1}$ and $v_{q,j}^{n+1,k}$ becomes negligible for all q and j. If this iteration does not converge, our scheme breaks down, or otherwise we would have all the $v_{q,j}^{n+1}$ once the iteration converges and then compute $v_{q,j}^{n+2}$.

A.2.1. Boundary condition.

A.2.1.1. Assumption of the total amount of asset. Using the boundary conditions mentioned at the beginning of the appendix, we can construct discretized equations at the boundaries. For $q=Q$, the discretized equation becomes

$$
\begin{aligned}
& v_{Q,j}^{n+1,k+1}[1+\frac{\Delta\tau}{\Delta s^2}\sigma^2-(\mu-s)\frac{\Delta\tau}{\Delta s}(1_{\mu<s}-1_{\mu>s})] \\
& +v_{Q,j+1}^{n+1,k+1}\left(-\frac{\Delta\tau}{2\Delta s^2}\sigma^2-(\mu-s)\frac{\Delta\tau}{\Delta s}1_{\mu>s}\right) \\
& +v_{Q,j-1}^{n+1,k+1}\left(-\frac{\Delta\tau}{2\Delta s^2}\sigma^2+(\mu-s)\frac{\Delta\tau}{\Delta s}1_{\mu<s}\right) \\
& =v_{Q,j}^{n}-\frac{\sigma^2}{2}\frac{\Delta\tau}{4\Delta s^2}\left(v_{Q,j+1}^{n+1,k}-v_{Q,j-1}^{n+1,k}\right)^2+\frac{A\Delta\tau}{\kappa+1}\left(1+\frac{1}{\kappa}\right)^{-\kappa}e^{-\kappa\left(-s-v_{Q-1,j}^{n+1,k}+v_{Q,j}^{n+1,k}\right)},
\end{aligned}
\tag{119}
$$

and for $q=-Q$, the discretized equation is

$$
\begin{aligned}
& v_{-Q,j}^{n+1,k+1}[1+\frac{\Delta\tau}{\Delta s^2}\sigma^2-(\mu-s)\frac{\Delta\tau}{\Delta s}(1_{\mu<s}-1_{\mu>s})] \\
& +v_{-Q,j+1}^{n+1,k+1}\left(-\frac{\Delta\tau}{2\Delta s^2}\sigma^2-(\mu-s)\frac{\Delta\tau}{\Delta s}1_{\mu>s}\right) \\
& +v_{-Q,j-1}^{n+1,k+1}\left(-\frac{\Delta\tau}{2\Delta s^2}\sigma^2+(\mu-s)\frac{\Delta\tau}{\Delta s}1_{\mu<s}\right) \\
& =v_{-Q,j}^{n}-\frac{\sigma^2}{2}\frac{\Delta\tau}{4\Delta s^2}\left(v_{-Q,j+1}^{n+1,k}-v_{-Q,j-1}^{n+1,k}\right)^2+\frac{A\Delta\tau}{\kappa+1}\left(1+\frac{1}{\kappa}\right)^{-\kappa}e^{-\kappa\left(s-v_{-Q+1,j}^{n+1,k}+v_{-Q,j}^{n+1,k}\right)}.
\end{aligned}
\tag{120}
$$

A.2.1.2. Zero second-derivatives at boundaries. We also try the following set of boundary conditions for the finite difference method, which is exact at the terminal time.

$$
\begin{aligned}
v^n_{Q,j} - v^n_{Q-1,j} &= v^n_{Q-1,j} - v^n_{Q-2,j} \\
v^n_{-Q,j} - v^n_{-Q+1,j} &= v^n_{-Q+1,j} - v^n_{-Q+2,j}
\end{aligned} \tag{121}
$$

From our experiments on the finite difference method with different boundary conditions, we observe that

(1) Different boundary conditions will eventually have an impact on the solution even at points away from the boundaries when T is sufficiently large.

(2) The "Zero second-derivative" boundary condition would "push" the optimal limit prices to constants, while the boundary condition derived from the assumption of the total amount of asset would "prevent" the optimal limit prices from converging to constants.

(3) To observe the "true" phenomena when time is far away from terminal, we need to set the space of inventory large enough. In our experiments, when we set the numerical boundaries for inventory to be ± 1000, the results from finite difference method using different boundary conditions match very well for q between ± 300, and they both indicate the same convergence of the optimal limit prices when time is away from terminal.

A.3. Split-step method. We make a change of variables $u(t,q,x,s) = -e^{-x}\tilde{v}(t,s,q)$ for u in (8). Then $\tilde{v}(t,s,q)$ satisfies, for $-Q < q < Q$,

$$
\tilde{v}_t(t,s,q) + (\mu - s)\tilde{v}_s(t,s,q) + \frac{1}{2}\sigma^2\tilde{v}_{ss}(t,s,q) - \frac{A}{\kappa+1}\left(e^{-\kappa\delta^b} + e^{-\kappa\delta^a}\right)\tilde{v}(t,s,q) = 0 \tag{122}
$$

and, for $q = \pm Q$,

$$
\tilde{v}_t(t,s,-Q) + (\mu - s)\tilde{v}_s(t,s,-Q) + \frac{1}{2}\sigma^2\tilde{v}_{ss}(t,s,-Q) - \frac{A}{\kappa+1}e^{-\kappa\delta^b}\tilde{v}(t,s,-Q) = 0 \tag{123}
$$

$$
\tilde{v}_t(t,s,Q) + (\mu - s)\tilde{v}_s(t,s,Q) + \frac{1}{2}\sigma^2\tilde{v}_{ss}(t,s,Q) - \frac{A}{\kappa+1}e^{-\kappa\delta^a}\tilde{v}(t,s,Q) = 0 \tag{124}
$$

with the optimal feedback control

$$
\begin{aligned}
\delta^b(t,s,q) &= s + \left[\log\left(1+\frac{1}{k}\right) + \log\tilde{v}(t,s,q+1) - \log\tilde{v}(t,s,q)\right] \\
\delta^a(t,s,q) &= -s + \left[\log\left(1+\frac{1}{k}\right) + \log\tilde{v}(t,s,q-1) - \log\tilde{v}(t,s,q)\right],
\end{aligned}
$$

Here the terminal condition is given by $\tilde{v}(T,s,q) = e^{-sq}$.

To solve $\tilde{v}(t,s,q)$ numerically, we use the split-step method that is a popular technique to numerically solve non-linear Schrödinger equations. Let

$$
\vec{v}(t,s) = (\tilde{v}(t,s,-Q), \tilde{v}(t,s,-Q+1), \ldots, \tilde{v}(t,s,Q-1), \tilde{v}(t,s,Q))^T. \tag{125}
$$

Then the evolution equation for $\tilde{v}(t,s,q)$ can be written as

$$\vec{v}_t(t,s) + \mathcal{S}\vec{v}(t,s) + \mathcal{Q}\vec{v}(t,s) = 0, \tag{126}$$

where $\mathcal{S}$ and $\mathcal{Q}$ are operators applied to $\vec{v}$:

$$\mathcal{S}\vec{v}(t,s) = \left[(\mu - s)\frac{\partial}{\partial s} + \frac{1}{2}\sigma^2\frac{\partial^2}{\partial s^2}\right]\vec{v}(t,s) \tag{127}$$

$$\mathcal{Q}\vec{v}(t,s) = -\frac{A}{\kappa+1}\begin{pmatrix} e^{-\kappa\delta^b}\tilde{v}(t,s,-Q) \\ (e^{-\kappa\delta^a} + e^{-\kappa\delta^b})\tilde{v}(t,s,-Q+1) \\ \vdots \\ (e^{-\kappa\delta^a} + e^{-\kappa\delta^b})\tilde{v}(t,s,Q-1) \\ e^{-\kappa\delta^a}\tilde{v}(t,s,Q) \end{pmatrix} \tag{128}$$

The idea of the split-step method is to solve the $\mathcal{S}$ and $\mathcal{Q}$ evolutions separately:

$$\vec{v}_t(t,s) + \mathcal{Q}\vec{v}(t,s) = 0, \quad \vec{v}_t(t,s) + \mathcal{S}\vec{v}(t,s) = 0, \tag{129}$$

The formal solutions to the separate evolution equations are $\vec{v}(t,s) = e^{(T-t)\mathcal{Q}}\vec{v}(T,s)$ and $\vec{v}(t,s) = e^{(T-t)\mathcal{S}}\vec{v}(T,s)$, respectively. For each time step, we first consider the $\mathcal{Q}$ evolution and then consider the $\mathcal{S}$ evolution. The formal solution of such a scheme is then given by

$$\vec{v}(t_{n+\frac{1}{2}},s) = e^{-\Delta t\mathcal{Q}}\vec{v}(t_{n+1},s), \quad \vec{v}(t_n,s) = e^{-\Delta t\mathcal{S}}\vec{v}(t_{n+\frac{1}{2}},s), \tag{130}$$

or equivalently,

$$\vec{v}(t_n,s) = e^{-\Delta t\mathcal{S}}e^{-\Delta t\mathcal{Q}}\vec{v}(t_{n+1},s), \tag{131}$$

and we expect that $\vec{v}(t_n,s)$ converges to the real solution as $\Delta t \to 0$.

The advantage of the split-step method is that we are able to easily compute the evolution operators $\mathcal{S}$ and $\mathcal{Q}$ and, therefore, we can numerically solve the full evolution equation effectively.

A.3.1. The $\mathcal{Q}$ evolution. We first consider the $\mathcal{Q}$ evolution: $\vec{v}_t(t,s) + \mathcal{Q}\vec{v}(t,s) = 0$. Here we note that the evolution equation is a special case of the Avellaneda and Stoikov model [3]. Therefore, we can find the exact solution by the technique described in [30, 52]. Let $w(t,s,q) = e^{-\kappa sq}\tilde{v}^{-\kappa}(t,s,q)$, then w satisfies

$$w_t(t,s,q) + \frac{A\kappa}{\kappa+1}\left(1+\frac{1}{\kappa}\right)^{-\kappa}[w(t,s,q-1) + w(t,s,q+1)] = 0, \quad -Q < q < Q \tag{132}$$

$$w_t(t,s,-Q) + \frac{A\kappa}{\kappa+1}\left(1+\frac{1}{\kappa}\right)^{-\kappa}w(t,s,-Q+1) = 0 \tag{133}$$

$$w_t(t,s,Q) + \frac{A\kappa}{\kappa+1}\left(1+\frac{1}{\kappa}\right)^{-\kappa}w(t,s,Q-1) = 0. \tag{134}$$

The above equations are solvable and for a fixed s,

$$\vec{w}(t,s) = e^{\Delta t M}\vec{w}(t+\Delta t, s),$$

where $\vec{w}(t,s) = (w(t,s,-Q), w(t,s,-Q+1), \ldots, w(t,s,Q-1), w(t,s,Q))^T$ and M is a tridiagonal matrix:

$$M = \frac{A\kappa}{\kappa+1}\left(1+\frac{1}{\kappa}\right)^{-\kappa}\begin{pmatrix} 0 & 1 & & & \\ 1 & \ddots & \ddots & & \\ & \ddots & \ddots & \ddots & \\ & & \ddots & \ddots & 1 \\ & & & 1 & 0 \end{pmatrix}. \tag{135}$$

Then $\tilde{v}(t,s,q) = e^{-sq}w^{-\frac{1}{\kappa}}(t,s,q)$.

A.3.2. The $\mathcal{S}$ evolution. We now consider the $\mathcal{S}$ evolution: $\vec{v}_t(t,s) + \mathcal{S}\vec{v}(t,s) = 0$. Note that $\mathcal{S}$ is an OU operator. Therefore, by the Feynman-Kac formula,

$$\tilde{v}(t,s,q) = \mathbb{E}[\tilde{v}(t+\Delta t, S_{t+\Delta t}, q)|S_t = s], \quad dS_t = (\mu - S_t)dt + \sigma dW_t, \tag{136}$$

where W_t is a Brownian motion.

To compute the numerical expectation, We discretize the s domain uniformly: $S_{\min} = s_1, s_2, \ldots, s_{N-1}, s_N = S_{\max}$ and $s_{i+1} - s_i = \Delta s$, and let

$$\tilde{v}(t,s_i,q) = \sum_{j=1}^{N} p_{ij}\tilde{v}(t+\Delta t, s_j, q) \tag{137}$$

$$p_{ij} = \mathbb{P}(s_j - \Delta S/2 < S_{t+\Delta t} \le s_j + \Delta S/2 | S_t = s), \quad 2 \le j \le N-1 \tag{138}$$

$$p_{i1} = \mathbb{P}(S_{t+\Delta t} \le s_1 + \Delta S/2 | S_t = s), \quad p_{iN} = \mathbb{P}(s_N - \Delta S/2 < S_{t+\Delta t} | S_t = s). \tag{139}$$

Given that $S_t = s$, $S_{t+\Delta t}$ is a Gaussian random variable with mean $e^{-\Delta t}s + (1-e^{-\Delta t})\mu$ and variance $\frac{\sigma^2}{2}(1-e^{-2\Delta t})$, we can easily compute the numerical values of p_{ij}.

Here we approximate the OU process S_t by a discrete time, discrete space Markov chain. To ensure the accuracy of the numerical expectation, we compare the stationary distributions of S_t and the Markov chain, and we calibrate Δs and Δt so that those two stationary distributions are close. To do that, we first select a reasonable step-size Δt for the time space (in our experiments, we typically choose 1/10 or 1/100 of the mean reversion time). Then we choose a sufficiently small Δs such that the difference between the two stationary distributions are negligible.

A.3.3. Scaling invariance and normalization of a solution. We observe that $\tilde{v}(t,s,q)$ is an exponential function of $T-t$. Thus, to see the long time behavior of $\tilde{v}(t,s,q)$ numerically, we will encounter the issue of the numerical overflow or underflow. We can avoid this issue by using the scaling invariance property of the HJB equation. From the differential equation of $\tilde{v}(t,s,q)$ (see (122)-(123)), we see that if $\tilde{v}(t,s,q)$ is a solution of the PDE with the terminal

condition $\tilde{v}(T,s,q)$, then for any positive constant c, $\tilde{v}(t,s,q)/c$ is also a solution of the PDE with the terminal condition $\tilde{v}(T,s,q)/c$. In addition, the optimal controls δ^b and δ^a are invariant for any $c>0$.

We can easily observe that the split-step method also preserves the scaling invariance property. Therefore, for each time step t_n, we can normalize the numerical solution by taking $\tilde{v}(t_n,s_i,q)/c_n$ with an appropriate constant $c_n>0$. To avoid numerical overflow and underflow, the best c_n is the square root of the product of the maximum and minimum of $\tilde{v}(t_n,s_i,q)$:

$$c_n=\sqrt{v^n_{\max}v^n_{\min}},\quad v^n_{\max}=\max_{s_i,q}\tilde{v}(t_n,s_i,q),\quad v^n_{\min}=\min_{s_i,q}\tilde{v}(t_n,s_i,q). \tag{140}$$

In addition, it is easy to observe that the numerical optimal control δ^b and δ^a are not affected by the normalization.

Appendix B. Asymptotic analysis in Gueant, Lehalle, and Fernandez-Tapia [30]. For completeness, we state the results of the asymptotic analysis in Gueant, Lehalle, and Fernandez-Tapia [30].

Consider the Avellaneda and Stoikov model

$$\begin{cases} dQ_t=dQ^b_t-dQ^a_t\\ dX_t=\left(S_t+\delta^a_t\right)dQ^a_t-\left(S_t-\delta^b_t\right)dQ^b_t\\ dS_t=\sigma dB_t\\ Q^b_t\sim \text{Poi}\left(Ae^{-\kappa\delta^b_t}\right)\\ Q^a_t\sim \text{Poi}\left(Ae^{-\kappa\delta^a_t}\right)\\ \sup\limits_{\delta^a,\delta^b}E\left[-e^{-\gamma(X_T+S_TQ_T)}\right]. \end{cases} \tag{141}$$

with a finite inventory space $\{-Q,\cdots,Q\}$. The value function is defined as

$$u\left(t,q,x,s\right)=\sup_{\delta^a,\delta^b}E\left(-e^{-\gamma W_T}|Q_t=q,X_t=x,S_t=s\right), \tag{142}$$

and the HJB equations for value function are:

For $|q|<Q$,

$$\begin{aligned} 0=u_t+\frac{\sigma^2}{2}u_{ss}+\max_{\delta^a,\delta^b}\Big\{&\\ &\left[u\left(t,q-1,x+s+\delta^a,s\right)-u\left(t,q,x,s\right)\right]Ae^{-\kappa\delta^a}+\\ &\left[u\left(t,q+1,x-s+\delta^b,s\right)-u\left(t,q,x,s\right)\right]Ae^{-\kappa\delta^b}\Big\} \end{aligned} \tag{143}$$

For $q=Q$,

$$0=u_t+\frac{\sigma^2}{2}u_{ss}+\max_{\delta^a}\left\{\left[u\left(t,q-1,x+s+\delta^a,s\right)-u\left(t,q,x,s\right)\right]Ae^{-\kappa\delta^a}\right\} \tag{144}$$

For $q = -Q$,

$$0 = u_t + \frac{\sigma^2}{2} u_{ss} + \max_{\delta^b} \left\{ \left[u\left(t, q+1, x-s+\delta^b, s\right) - u\left(t,q,x,s\right) \right] A e^{-\kappa \delta^b} \right\} \tag{145}$$

with the terminal condition:

$$u\left(T, q, x, s\right) = -e^{-\gamma(x+qs)}, \quad \forall q \in \{-Q, \cdots, Q\}. \tag{146}$$

The optimal spreads are given by

$$\begin{aligned} \delta^{b*}\left(t,q\right) &= \frac{1}{\kappa} \log\left(\frac{v\left(t,q\right)}{v\left(t,q+1\right)}\right) + \frac{1}{\gamma} \log\left(1+\frac{\gamma}{\kappa}\right) \quad q \neq Q \\ \delta^{a*}\left(t,q\right) &= \frac{1}{\kappa} \log\left(\frac{v\left(t,q\right)}{v\left(t,q-1\right)}\right) + \frac{1}{\gamma} \log\left(1+\frac{\gamma}{\kappa}\right) \quad q \neq Q, \end{aligned} \tag{147}$$

where $v\left(t,q\right)$ is an ansatz satisfying

$$u(t,x,q,s) = -e^{-\gamma(x+qs)} v\left(t,q\right)^{-\frac{\gamma}{\kappa}}. \tag{148}$$

The asymptotic result is that

$$\begin{aligned} \lim_{T\to\infty} \delta^{b*}\left(0,q\right) &= \frac{1}{\gamma} \log\left(1+\frac{\gamma}{\kappa}\right) + \frac{1}{\kappa} \log\left(\frac{f_q^0}{f_{q+1}^0}\right) \\ \lim_{T\to\infty} \delta^{a*}\left(0,q\right) &= \frac{1}{\gamma} \log\left(1+\frac{\gamma}{\kappa}\right) + \frac{1}{\kappa} \log\left(\frac{f_q^0}{f_{q-1}^0}\right) \end{aligned} \tag{149}$$

where $f^0 \in \mathbb{R}^{2Q+1}$ is an eigenvector corresponding to the smallest eigenvalue of the matrix M defined by

$$\begin{bmatrix} \alpha Q^2 & -\eta & 0 & \cdots & \cdots & \cdots & 0 \\ -\eta & \alpha(Q-1)^2 & -\eta & 0 & \ddots & \ddots & \vdots \\ \vdots & \ddots & \ddots & \ddots & \ddots & \ddots & \vdots \\ 0 & \ddots & \ddots & 0 & -\eta & \alpha(Q-1)^2 & -\eta \\ 0 & \cdots & \cdots & \cdots & 0 & -\eta & \alpha Q^2 \end{bmatrix}$$

with $\alpha = \frac{\kappa}{2}\gamma\sigma^2$ and $\eta = A\left(1+\frac{\gamma}{\kappa}\right)^{-\left(1+\frac{\kappa}{\gamma}\right)}$. We refer to Theorem 1 and Theorem 2 in [30] for more detail.

REFERENCES

[1] A. Alfonsi, A. Fruth, and A. Schied, *Optimal execution strategies in limit order books with general shape functions*, Quantitative Finance, 10 (2010), pp. 143–157.

[2] R. Almgren and N. Chriss, *Optimal execution of portfolio transactions*, Journal of Risk, (2001), pp. 5–39.

[3] M. Avellaneda and S. Stoikov, *High-frequency trading in a limit order book*, Quantitative Finance, 8 (2008), pp. 217–224.
[4] E. Bandini and M. Fuhrman, *Constrained bsdes representation of the value function in optimal control of pure jump markov processes.*
[5] N. Bäuerle and U. Rieder, *Mdp algorithms for portfolio optimization problems in pure jump markets*, Finance and Stochastics, 13 (2009), pp. 591–611.
[6] E. Bayraktar and M. Ludkovski, *Liquidation in limit order books with controlled intensity*, Mathematical Finance, 24 (2014), pp. 627–650.
[7] J. Berkowitz, *On the discreteness of spectra of singular sturm-liouville problems*, Communications on Pure and Applied Mathematics, 12 (1959), pp. 523–542.
[8] J.-P. Bouchaud, *Price impact*, Entry of "Encyclopedia of Quantitative Finance", (2009).
[9] J.-P. Bouchaud, Y. Gefen, M. Potters, and M. Wyart, *Fluctuations and response in financial markets: the subtle nature of 'random' price changes*, Quantitative Finance, (2003).
[10] J.-P. Bouchaud, M. Mezard, and M. Potters, *Statistical properties of stock order books: empirical results and models*, Science & Finance (CFM) working paper archive 0203511, Science & Finance, Capital Fund Management, Mar. 2002.
[11] J.-P. Bouchaud, M. MÉzard, and M. Potters, *Statistical properties of stock order books: empirical results and models*, Quantitative Finance, 2 (2002), pp. 251–256.
[12] P. Cardaliaguet, J.-M. Lasry, P.-L. Lions, and A. Porretta, *Long time average of mean field games with a nonlocal coupling*, SIAM Journal on Control and Optimization, 51 (2013), pp. 3558–3591.
[13] P. Cardaliaguet, J.-M. Lasry, P.-L. Lions, A. Porretta, et al., *Long time average of mean field games.*, NHM, 7 (2012), pp. 279–301.
[14] R. Carmona and J. Yang, *Predatory trading: a gmae on volatility and liquidity*, (2011).
[15] Á. Cartea, S. Jaimungal, and J. Ricci, *Buy low, sell high: A high frequency trading perspective*, SIAM Journal on Financial Mathematics, 5 (2014), pp. 415–444.
[16] R. Cont, A. Kukanov, and S. Stoikov, *The price impact of order book events*, Journal of Financial Econometrics, (2013).
[17] R. Cont, S. Stoikov, and R. Talreja, *A stochastic model for order book dynamics*, Operations Research, 58 (2010), pp. 549–563.
[18] F. Delarue and S. Menozzi, *A forward?backward stochastic algorithm for quasi-linear pdes*, Ann. Appl. Probab., 16 (2006), pp. 140–184.
[19] P. Fodra and M. Labadie, *High-frequency market-making with inventory constraints and directional bets*, Working Papers hal-00675925, HAL, Mar. 2012.
[20] ———, *High-frequency market-making for multi-dimensional Markov processes*, ArXiv e-prints, (2013).
[21] J. Fouque, G. Papanicolaou, and K. Sircar, *Derivatives in Financial Markets with Stochastic Volatility*, Cambridge University Press, 2000.
[22] J. Fouque, G. Papanicolaou, R. Sircar, and K. Sølna, *Multiscale Stochastic Volatility for Equity, Interest Rate, and Credit Derivatives*, Cambridge University Press, 2011.
[23] N. Framstad, B. Øksendal, and A. Sulem, *Sufficient stochastic maximum principle for the optimal control of jump diffusions and applications to finance*, Journal of Optimization Theory and Applications, 121 (2004), pp. 77–98.
[24] M. Fuhrman and H. Pham, *Randomized and backward sde representation for optimal control of non-markovian sdes*, Ann. Appl. Probab., 25 (2015), pp. 2134–2167.
[25] X. Gabaix, P. Gopikrishnan, V. Plerou, and H. E. Stanley, *Institutional investors and stock market volatility.*, Quarterly Journal of Economics, 121 (2006).
[26] J. Gatheral, *No-dynamic-arbitrage and market impact*, Quantitative Finance, 10 (2010), pp. 749–759.
[27] P. Gopikrishnan, V. Plerou, X. Gabaix, and H. E. Stanley, *Statistical properties of share volume traded in financial markets*, Phys. Rev. E, 62 (2000), pp. R4493–R4496.
[28] M. D. Gould, M. A. Porter, S. Williams, M. McDonald, D. J. Fenn, and S. D. Howison, *Limit order books*, Quantitative Finance, 13 (2013), pp. 1709–1742.
[29] O. Guéant, C. Lehalle, and J. Fernandez-Tapia, *Optimal portfolio liquidation with limit orders*, SIAM Journal on Financial Mathematics, 3 (2012), pp. 740–764.
[30] ———, *Dealing with the inventory risk: a solution to the market making problem*, Mathematics and

Financial Economics, 7 (2013), pp. 477–507.
[31] O. Gueant and C.-A. Lehalle, *General intensity shapes in optimal liquidation*, Mathematical Finance, 25 (2015), pp. 457–495.
[32] F. Guilbaud and H. Pham, *Optimal high-frequency trading with limit and market orders*, Quantitative Finance, 13 (2013), pp. 79–94.
[33] E. Hillebrand, *Mean Reversion Models of Financial Markets*, PhD thesis, University of Bremen, 2003.
[34] ———, *Neglecting parameter changes in GARCH models*, Journal of Econometrics, 129 (2005), pp. 121 – 138.
[35] T. Ho and H. R. Stoll, *On Dealer Markets under Competition*, Journal of Finance, 35 (1980), pp. 259–67.
[36] G. Huberman and W. Stanzl, *Quasi-arbitrage and price manipulation ???*, 2001.
[37] I. Kharroubi, N. Langrené, and H. Pham, *A numerical algorithm for fully nonlinear HJB equations: An approach by control randomization*, Monte Carlo Methods and Applications, 20 (2014), pp. 145–165.
[38] C. Krauss, *Statistical arbitrage pairs trading strategies: Review and outlook*, IWQW Discussion Paper Series 09/2015, 2015.
[39] S. E. Ludwig, *Optimal portfolio allocation of commodity related assets using a controlled forward-backward stochastic algorithm*, PhD thesis, University of Heidelberg, 2013.
[40] S. Maslov and M. Mills, *Price fluctuations from the order book perspective?empirical facts and a simple model*, Physica A: Statistical Mechanics and its Applications, 299 (2001), pp. 234–246.
[41] A. Mendoza, H. Waelbroeck, and C. R. Stephens, *Relating market impact to aggregate order flow: The role of supply and demand in explaining concavity and order flow dynamics*, (2009).
[42] A. A. Obizhaeva and J. Wang, *Optimal trading strategy and supply/demand dynamics*, Journal of Financial Markets, 16 (2013), pp. 1–32.
[43] G. Pagès and J. Printems, *Optimal quadratic quantization for numerics: the gaussian case*, Monte Carlo Methods and Applications, 9 (2003), p. 135–166.
[44] A. Pankov, *Introduction to spectral theory of schrödinger operators*, Lecture Notes), Preprint, Giessen University, (2001).
[45] C. A. Parlour and D. J. Seppi, *Limit order markets : a survey*, Handbook of financial intermediation and banking., (2008).
[46] H. Pham, *Feynman-kac representation of fully nonlinear pdes and applications*, Acta Mathematica Vietnamica, 40 (2015), pp. 255–269.
[47] M. Potters and J.-P. Bouchaud, *More statistical properties of order books and price impact*, Physica A: Statistical Mechanics and its Applications, 324 (2003), pp. 133–140.
[48] M. Razavy, *An exactly soluble schrödinger equation with a bistable potential*, American Journal of Physics, 48 (1980), pp. 285–288.
[49] A. Schied and T. Zhang, *A state-constrained differential game arising in optimal portfolio liquidation*, Mathematical Finance, (2015).
[50] E. Smith, J. D. Farmer, L. Gillemot, and S. Krishnamurthy, *Statistical theory of the continuous double auction*, Quantitative Finance, 3 (2003), pp. 481–514.
[51] P. Weber and B. Rosenow, *Order book approach to price impact*, Quantitative Finance, 5 (2005), pp. 357–364.
[52] K. Zhang, *Two Problems in Quantitative Finance*, PhD thesis, Stanford University, Stanford, CA, 2009.